

Latent Gaussian dynamic factor modeling and forecasting for multivariate count time series

Younghoon Kim¹, Zachary F. Fisher², and Vladas Pipiras³

¹Cornell University

²University of North Carolina at Chapel Hill

³The Pennsylvania State University

July 21, 2023

Abstract

This work considers estimation and forecasting in a multivariate count time series model based on a copula-type transformation of a Gaussian dynamic factor model. The estimation is based on second-order properties of the count and underlying Gaussian models and applies to the case where the model dimension is larger than the sample length. In addition, novel cross-validation schemes are suggested for model selection. The forecasting is carried out through a particle-based sequential Monte Carlo, leveraging Kalman filtering techniques. A simulation study and an application are also considered.

Keywords— Count time series, dynamic factor model, Hermite expansions, Yule-Walker equations, principle components, sequential Monte Carlo.

1 Introduction

This work develops theory, estimation, and forecasting methods for dynamic factor modeling of discrete-valued multivariate time series. Count time series are exceedingly common across the natural, health, and social sciences. Examples include monthly counts of earthquakes whose magnitude exceeds a certain threshold, daily counts of individuals infected with a virus, and minute-by-minute recordings of conversational interactions between two communicating partners. Specifically, we are interested in a d -vector time series $X_t = (X_{i,t})_{i=1,\dots,d}$, where $X_{i,t} \in \mathbb{N}_0 = \{0, 1, 2, \dots\}$ and $t \in \mathbb{Z}$ is

time. The considered model accommodates the range \mathbb{Z} easily as well but counts and the range \mathbb{N}_0 are encountered more commonly in practice. Note that any set of finite discrete values can also be encoded as a subset of \mathbb{N}_0 . The focus is on stationary models throughout, though the possibilities of covariates and differencing will also be considered.

In general, modeling time series with discrete (count) values is delicate. In the continuous case, the class of autoregressive moving average (ARMA) models parsimoniously spans all non-deterministic stationary series (by the classical Wold decomposition). In the count setting, the landscape is far less determined, with class of models dominating in popularity. In fact, researchers have devised many different methods for constructing stationary count time series. The majority of work on count time series has been devoted to the univariate case. Popular approaches include those based on thinning operators (e.g. McKenzie, 1985, Alzaid and Al-Osh, 1993) and the generalized state-space models (e.g. Davis et al., 2016), including Markov chain and Hidden Markov Models (HMMs), Bayesian dynamic models (e.g. Gamerman et al., 2016). Integer-valued autoregressive conditional heteroskedasticity modeling (e.g. Ferland et al., 2006, Fokianos et al., 2009) is another popular observation-driven approach. Recent reviews of this research area are given in Weiß (2018) and Davis et al. (2021).

Compared to univariate count series, the analysis of multivariate, and potentially high-dimensional, count series has received considerably less attention. For a review of approaches for multivariate counts, see Karlis (2016) and for recent work on generalized linear model (GLM) constructions in high-dimensional settings, see Chen et al. (2017), Hall et al. (2018), Mark et al. (2018, 2019), and Fokianos et al. (2020). Dynamic factor models for multivariate count time series have been considered by Jung et al. (2011), Cui and Dunson (2014), Wang and Wang (2018), and Bräuning and Koopman (2020) which posit conditional distributions akin to GLM in their likelihood maximization procedures. In a collection of articles on count time series, Karlis (2016) surveys relatively recent works on multivariate discrete-valued time series models.

In a recent paper, Jia et al. (2023) proposed a general Gaussian copula-based approach to model count series with a flexible and most general correlation structure that can accommodate any count marginal distribution. The marginal distribution can exhibit over- or under-dispersion, or have zero-inflation. The autocovariance function (ACVF) of the model is as general as possible for a given marginal distribution, capable of achieving the most negative pairwise correlations. In particular, the range of attainable correlations for this model can be obtained from the result of Whitt (1976). Kong and Lund (2023) further extended the model to incorporate periodic and seasonal features by

replacing the vanilla ARMA with periodic autoregressive moving average (PARMA) and seasonal autoregressive moving average (SARMA) models.

The goal of this work is to propose a multivariate extension of Jia et al. (2023) based on latent Gaussian dynamic factor models (DFMs) where the factors follow stationary vector autoregressive (VAR) models. The exact definition of our model is given in (1), (3) and (4) below. We propose new methods for estimating the dynamic factor model parameters and for forecasting with the estimated model. On the estimation side, our method can be applied when the dimension d is large, possibly much larger than the sample length itself. To make that possible, we exploit second-order properties of the count and underlying Gaussian models, in conjunction with principle component and Yule-Walker estimation. We additionally suggest novel cross-validation schemes related to model selection, namely, the number of factor series and the lag order in their VAR model. We expect our proposed estimators to be consistent in theory based on recent results from Düker et al. (2023) but the proof of consistency goes beyond the scope of this work and will appear elsewhere (see Remark 3.2 below). The forecasting is carried out through a particle-based sequential Monte Carlo method, leveraging Kalman filtering techniques. Lastly, the modeling and forecasting approach is illustrated on real psychometrics data. With these data, we find the model interpretation and the understanding of forecasting issues particularly interesting and informative.

In psychometrics, latent factor models for discrete-valued data have been in increasing demand because of the abundance of such categorical data, and an expectation for them to be explained by the several presumed latent factors (e.g. Lebo and Nesselroade, 1978). The most common approach is based on polychoric correlations (e.g. Muthén, 1984) with implementations in various structural equation modeling software, including the popular R package `lavaan` (Rosseel, 2012). In time series and Bayesian context, Zhang and Nesselroade (2007) and Zhang and Browne (2010) introduced a categorical dynamic factor model. These approaches are based on the discretization of Gaussian variables through thresholding, akin to the modeling approach taken here. However, the estimation methods are not well-suited to higher-dimensional settings, or time-dependent data more generally, where forecasting may be of interest. We refer readers to Robitzsch (2020) for a review of this approach to the factor analysis of ordinal data in psychometrics.

In summary, our main contributions and highlights of the paper are as follows:

- The introduction of a dynamic factor model for multivariate discrete-valued time series.
- The proposal of a relatively simple approach to parameter estimation, for which theoretical

foundations are laid elsewhere.

- The development of forecasting schemes specific to the discrete nature of the model and time series data.
- An instructive application to psychometrics showcasing the model and forecasting appeal in terms of interpretability and flexibility.

The rest of the paper is organized as follows. Section 2 introduces the latent Gaussian dynamic factor model and establishes relationships between the second-order dependence structures of count and underlying Gaussian models. The estimation procedure is provided in Section 3. Section 4 discusses forecasting. Numerical experiments can be found in Section 5, followed by an illustrative application in Section 6. We close our paper with comments for future work in Section 7.

2 Latent Gaussian dynamic factor model

2.1 Model formulation

For a d -vector time series $\{X_t\}_{t \in \mathbb{Z}} = \{(X_{i,t})_{i=1,\dots,d}\}_{t \in \mathbb{Z}}$, a latent Gaussian dynamic factor model is defined as follows. For $i = 1, \dots, d$, each component series $X_{i,t}$ is given by

$$X_{i,t} = F_i^{-1}(\Phi(Z_{i,t})) =: G_i(Z_{i,t}), \quad (1)$$

where F_i is a CDF, $F_i^{-1}(u) = \inf\{v : F_i(v) \geq u\}$ is its (generalized) inverse, $\Phi(z)$ is the CDF of $\mathcal{N}(0, 1)$ distribution, and $Z_{i,t}$ is a zero mean, unit variance, Gaussian stationary series defined below. The CDFs F_i are thought to come from parametric families, parameterized by a (possibly vector) parameter θ_i . Note that by construction (1), $X_{i,t}$ is a stationary series and its marginal distribution is F_i . We focus here on discrete distributions F_i taking nonnegative integer values \mathbb{N}_0 such as Bernoulli, Poisson, negative binomial, and so on. For example, if F_i is the CDF of a Bernoulli distribution with parameter p_i , $\text{Bern}(p_i)$ for short, the model (1) becomes $X_{i,t} = 1_{\{\Phi(Z_{i,t}) > 1-p_i\}} = 1_{\{Z_{i,t} > \Phi^{-1}(1-p_i)\}}$. More generally, if F_i is a CDF whose support lies in \mathbb{N}_0 , for example a Poisson distribution with parameter λ_i , then $X_{i,t}$ is represented through $Z_{i,t}$ by

$$X_{i,t} = \sum_{n=1}^{\infty} n 1_{\{\Phi^{-1}(C_{i,n-1}) < Z_{i,t} \leq \Phi^{-1}(C_{i,n})\}}, \quad C_{i,n} = \mathbb{P}(X_{i,t} \leq n) = F_i(n), \quad n = 0, 1, \dots \quad (2)$$

In fact, (2) defines a count random variable $X_{i,t}$ represented through $Z_{i,t}$ that follows any marginal distribution F_i . However, we shall use the examples of Bernoulli, Poisson, and negative binomial marginal distributions for illustration throughout the paper. Whereas the Poisson distribution with a large parameter is close to Gaussian and the latent $Z_{i,t}$'s are effectively observed, note that the Bernoulli case lies at the other extreme and is expected to be most difficult to deal with in our tasks. Additionally, our model (2) can allow parameters θ_i to vary over time, wherein the bins $(\Phi^{-1}(C_{i,n-1}), \Phi^{-1}(C_{i,n})]$ for $Z_{i,t}$ can depend on time. This leads to nonstationary models which will be discussed briefly below.

We are interested in the scenario where the underlying Gaussian series $Z_{i,t}$ obeys a DFM. More specifically, we suppose that the d -vector time series $Z_t = (Z_{i,t})_{i=1,\dots,d}$ satisfies

$$Z_t = \Lambda Y_t + \varepsilon_t, \quad (3)$$

where Λ is a $d \times r$ loadings matrix, and ε_t are i.i.d. $\mathcal{N}(0, \Sigma_\varepsilon)$ random d -vectors (independent of Y_t 's) and r -vector factor series $Y_t = (Y_{k,t})_{k=1,\dots,r}$ follows a stationary VAR model of order p , VAR(p) for short, given by

$$Y_t = \Psi_1 Y_{t-1} + \dots + \Psi_p Y_{t-p} + \eta_t, \quad (4)$$

where Ψ_1, \dots, Ψ_p are $r \times r$ matrices and η_t are i.i.d. $\mathcal{N}(0, \Sigma_\eta)$ random r -vectors. The VAR model (4) is flexible to capture any temporal dependence from a practical standpoint. Note that the DFM (3) is in the so-called static form. The generalized DFMs where (3) includes lags of Y_t (e.g. Forni et al., 2000, 2005) go beyond the scope of this work.

Note that the unit variance of $Z_{i,t}$ is assumed in (1). For general $Z_{i,t}$, one can standardize it to have unit variance. More generally, the autocovariance function (ACVF) $\Sigma_Z(h) = \mathbb{E}Z_{t+h}Z_t'$ of Z_t at lag h can similarly become autocorrelation function (ACF) $R_Z(h)$ as

$$R_Z(h) = \text{diag}(\Sigma_Z(0))^{-1/2} \Sigma_Z(h) \text{diag}(\Sigma_Z(0))^{-1/2}. \quad (5)$$

We use $R_Z(h)$ for the rest of the analysis so the unit variance assumption for $Z_{i,t}$ is made throughout.

2.2 Relation between count and Gaussian correlations

Our estimation procedure is based on the following property of the model (1). It is known (e.g. Pipiras and Taqqu, 2017) that, for any $i, j = 1, \dots, d$,

$$R_{X,ij}(h) = L_{ij}(R_{Z,ij}(h)) \quad (6)$$

or, in short, and entry-wise,

$$R_X(h) = L(R_Z(h)), \quad (7)$$

where $L_{ij} : [-1, 1] \mapsto [-1, 1]$ are functions to be referred to as link functions (and L as a link function). Furthermore, L_{ij} depends only on the CDFs F_i and F_j and can be expressed as described next.

For $k = 0, 1, \dots$, let $H_k(z) = (-1)^k e^{z^2/2} (d^k e^{-z^2/2} / dz^k)$ be the Hermite polynomial of order k and

$$g_{i,k} = \frac{1}{k!} \int_{-\infty}^{\infty} G_i(z) H_k(z) \frac{e^{-z^2/2}}{\sqrt{2\pi}} dz = \frac{1}{k!} \mathbb{E}[G_i(Z_{i,0}) H_k(Z_{i,0})] \quad (8)$$

be the corresponding Hermite coefficient of the function $G_i(z)$ in (1), so that $G_i(z) = \sum_{k=0}^{\infty} g_{i,k} H_k(z)$. For $G_i(z)$ associated with CDF F_i on nonnegative integers, Jia et al. (2023) showed that

$$g_{i,k} = \frac{1}{k! \sqrt{2\pi}} \sum_{n=0}^{\infty} e^{-\Phi^{-1}(C_{i,n})^2/2} H_{k-1}(\Phi^{-1}(C_{i,n})), \quad (9)$$

where $C_{i,n} = \mathbb{P}(X_{i,t} \leq n) = F_i(n)$. When $\Phi^{-1}(C_{i,n}) = \pm\infty$ for $C_{i,n} = 0$ or 1 , the summand $e^{-\Phi^{-1}(C_{i,n})^2/2} H_{k-1}(\Phi^{-1}(C_{i,n}))$ is interpreted as zero. For example, for $F_i = \text{Bern}(p_i)$, $g_{i,k} = e^{-\Phi^{-1}(p_i)^2/2} H_{k-1}(\Phi^{-1}(p_i)) / (k! \sqrt{2\pi})$. Similarly, $g_{i,k}$ can be computed when $F_i = \text{Pois}(\lambda_i)$ but (9) will have infinitely many terms. However, the number of terms will be finite and small in practice. This is because the Poisson distribution is light-tailed so that $C_{i,n}$ is indistinguishable from 1 numerically even at moderate n .

The link functions L_{ij} can now be expressed as

$$L_{ij}(u) = \sum_{k=1}^{\infty} \frac{k! g_{i,k} g_{j,k}}{\Sigma_{X,ii}(0)^{1/2} \Sigma_{X,jj}(0)^{1/2}} u^k =: \sum_{k=1}^{\infty} \ell_{ij,k} u^k. \quad (10)$$

Under mild assumptions, they can be shown to be monotonically increasing on the interval $(-1, 1)$ (see Proposition A.1. in the appendix of Jia et al., 2023). Note that $L_{ij}(0) = 0$ regardless of the

marginal distributions. The quantities $\rho_{+,ij} = L_{ij}(1)$ and $\rho_{-,ij} = L_{ij}(-1)$ are given by

$$\rho_{+,ij} = L_{ij}(1) = \text{Corr}(G_i(Z), G_j(Z)), \quad \rho_{-,ij} = L_{ij}(-1) = \text{Corr}(G_i(Z), G_j(-Z)) \quad (11)$$

for $Z = \mathcal{N}(0, 1)$. When $i = j$, $\rho_{+,ij} = 1$ but usually $\rho_{-,ij} > -1$. As noted in Jia et al. (2023), $\rho_{+,ij}$ and $\rho_{-,ij}$ are the largest and smallest correlations that two dependent count variables with marginals F_i and F_j can achieve; by (11), they are achieved with construction $G(Z)$ and hence within our considered model. For example, when $F_i = \text{Bern}(p_i)$, it can be shown by using (11) that

$$L_{ij}(1) = \begin{cases} \sqrt{\frac{p_i(1-p_j)}{p_j(1-p_i)}}, & \text{if } p_i \leq p_j, \\ \sqrt{\frac{p_j(1-p_i)}{p_i(1-p_j)}}, & \text{if } p_j < p_i, \end{cases} \quad L_{ij}(-1) = \begin{cases} -\sqrt{\frac{(1-p_i)(1-p_j)}{p_i p_j}}, & \text{if } p_i + p_j \geq 1, \\ -\sqrt{\frac{p_j p_i}{(1-p_i)(1-p_j)}}, & \text{if } p_i + p_j < 1. \end{cases} \quad (12)$$

Since the link functions L_{ij} are monotonically increasing, the inverse link functions can be defined as $L_{ij}^{-1} : [\rho_{-,ij}, \rho_{+,ij}] \mapsto [-1, 1]$. We will discuss the numerical calculation of the inverse L_{ij}^{-1} in Section 3.2 below. Thus, (6) and (7) imply that

$$R_{Z,ij}(h) = L_{ij}^{-1}(R_{X,ij}(h)) \quad (13)$$

or, in short and entrywise,

$$R_Z(h) = L^{-1}(R_X(h)). \quad (14)$$

2.3 Nonstationary models with covariates and differencing

As discussed in Jia et al. (2023), covariates can be incorporated easily into the model through its marginal parameters θ_i as follows. Suppose that $\theta_i(t)$ varies over time and is driven by J -dimensional deterministic covariate vector M_t as

$$\theta_i(t) = f(\beta_i' M_t), \quad (15)$$

where $\beta_i' M_t$ is a linear combination of a coefficient vector and the covariate, and f is a suitable function in the spirit of GLM. Then, the model (1) becomes

$$X_{i,t} = F_{i,\theta_i(t)}^{-1}(\Phi(Z_{i,t})) =: G_{i,\theta_i(t)}(Z_{i,t}). \quad (16)$$

This time-varying parameter leads to the cumulative distribution of $X_{i,t}$ as $C_{i,n}(t) = \mathbb{P}(X_{i,t} \leq n) = F_{i,\theta_i(t)}(n)$ and the computation of the Hermite coefficients in (9), now denoted by $g_{\theta_i(t),k}$, is still valid. The cross-correlation between X_{i,t_1} and X_{j,t_2} is represented by the cross-correlation between Z_{i,t_1} and Z_{j,t_2} as

$$R_{X,ij}(t_1 - t_2) = L_{\theta_i(t_1),\theta_j(t_2)}(R_{Z,ij}(t_1 - t_2)), \quad (17)$$

where, from (10),

$$L_{\theta_i(t_1),\theta_j(t_2)}(u) = \sum_{k=1}^{\infty} \frac{k! g_{\theta_i(t_1),k} g_{\theta_j(t_2),k}}{\text{Var}(X_{i,t})^{1/2} \text{Var}(X_{j,t})^{1/2}} u^k. \quad (18)$$

As we will see in Section 3.2, the numerical inverse of the link function is considered in the estimation. Although the computational burden is substantially increased with (18), the estimation is still feasible.

Another possibility to accommodate nonstationary with our model is to difference the count series $X_{i,t}$. That is, consider the series $\Delta X_{i,t} = X_{i,t} - X_{i,t-1}$, whose range now lies in \mathbb{Z} . As noted above, the considered model (1) may as well be defined on \mathbb{Z} , with a suitable choice of marginal distribution F_i (e.g. the Skellam distribution). Differencing of count time series and subsequent modeling of \mathbb{Z} -valued time series was considered by many researchers, including Kim and Park (2008), Zhang et al. (2010), Kachour and Truquet (2011), and others, but their models are generally non-trivial extension of the counterpart models for counts.

3 Estimation

3.1 Estimation with known link function

We describe here how the parameters $\Lambda, \Psi_1, \dots, \Psi_p, \Sigma_\epsilon$ and Σ_η with known r, p can be estimated assuming that the marginal CDFs F_i and the link functions L_{ij} are known. (The next sections will discuss estimation and computation of L_{ij} , and selection of r, p .) The basic idea is quite simple. Note that the relation (14) allows one to estimate $R_Z(h) = \Sigma_Z(h)$, $h = 0, \dots, p$, as

$$\hat{R}_Z(h) = L^{-1}(\hat{R}_X(h)), \quad (19)$$

where $\hat{R}_X(h)$ is the sample matrix ACF of the data X_1, \dots, X_T . $\hat{R}_X(h)$, $h \neq 0$, are not necessarily symmetric. Similarly, $\hat{R}_Z(0)$ is symmetric but not necessarily non-negative definite. The estimated covariance $\hat{R}_Z(0)$ of the latent Gaussian process will be used in forecasting described in the next

section. If needed, we employ a small positive shift of the eigenvalues to make $\hat{R}_Z(0)$ non-negative definite. However, we do not shift eigenvalues through the estimation procedure.

Since Z_t follows the dynamic factor model (3) and (4), the loadings matrix Λ , $\Sigma_Y(0)$, and Σ_ε can be estimated through principle components. More specifically, since the dynamic factor model (3) implies

$$R_Z(0) = \Lambda \Sigma_Y(0) \Lambda' + \Sigma_\varepsilon, \quad (20)$$

it is natural to estimate $\Lambda \Sigma_Y(0) \Lambda'$ as an r -rank approximation of $R_Z(0)$, and take Σ_ε as the approximation error. We thus proceed as follows. Let $\hat{R}_Z(0) = \hat{U} \hat{E} \hat{U}'$ be the eigendecomposition with $\hat{E} = \text{diag}(\hat{e}_1, \dots, \hat{e}_d)$ consisting of ordered eigenvalues $\hat{e}_1 \geq \dots \geq \hat{e}_d$, and $\hat{U} = (\hat{u}_1, \dots, \hat{u}_d)$ being the orthogonal eigenvector matrix. Setting $\hat{U}_r = (\hat{u}_1, \dots, \hat{u}_r)$ and $\hat{E}_r = \text{diag}(\hat{e}_1, \dots, \hat{e}_r)$, a rank- r approximation of $\Sigma_Z(0)$ can be taken as

$$\hat{U}_r \hat{E}_r \hat{U}_r' = (\hat{U}_r \hat{E}_r^{1/2})(\hat{U}_r \hat{E}_r^{1/2})'. \quad (21)$$

The relations (21) and (20) suggest setting

$$\hat{\Lambda} = \hat{U}_r, \quad \hat{\Sigma}_Y(0) = \hat{E}_r. \quad (22)$$

By construction, the choice (22) identifies $\Lambda, \Sigma_Y(0)$, after a possible non-singular $r \times r$ transformation, assuming that

$$\Lambda' \Lambda = I_r, \quad \Sigma_Y(0) = \text{diagonal}. \quad (23)$$

As in Bai and Wang (2015), another way to have identifiability for the DFM is to make the first $r \times r$ block of the loadings matrix be identity, that is,

$$\Lambda = \begin{pmatrix} I_r \\ \Lambda_2 \end{pmatrix}, \quad (24)$$

where Λ_2 is $(d - r) \times r$. We adopt the identification (24) for the rest of the paper.

Note that with the convention (24) above,

$$\Lambda \Sigma_Y(0) \Lambda' = \begin{pmatrix} \Sigma_Y(0) & \Sigma_Y(0) \Lambda_2' \\ \Lambda_2 \Sigma_Y(0) & \Lambda_2 \Sigma_Y(0) \Lambda_2' \end{pmatrix} = \begin{pmatrix} \Sigma_Y(0)^{1/2} \\ \Lambda_2 \Sigma_Y(0)^{1/2} \end{pmatrix} \begin{pmatrix} \Sigma_Y(0)^{1/2} & \Sigma_Y(0)^{1/2} \Lambda_2' \end{pmatrix}. \quad (25)$$

The relations (25) and (21) also suggest setting

$$\begin{pmatrix} \Sigma_Y(0)^{1/2} \\ \Lambda_2 \Sigma_Y(0)^{1/2} \end{pmatrix} = \hat{U}_r \hat{E}_r^{1/2} \quad (26)$$

to define both $\hat{\Sigma}_Y(0)^{1/2}$ and $\hat{\Lambda}_2$. Either (22) or (26) lead to estimators $\hat{\Lambda}$ and $\hat{\Sigma}_Y(0)$. The estimator $\hat{\Sigma}_\varepsilon$ can now be defined as

$$\hat{\Sigma}_\varepsilon = \hat{R}_Z(0) - \hat{U}_r \hat{E}_r \hat{U}_r' \quad (27)$$

Note also that DFM (3) yields

$$R_Z(h) = \Lambda \Sigma_Y(h) \Lambda', \quad h = 1, \dots, p. \quad (28)$$

Setting $\hat{R}_Z(h) = L^{-1}(\hat{R}_X(h))$ as in (19) naturally suggests the estimators

$$\hat{\Sigma}_Y(h) = (\hat{\Lambda}' \hat{\Lambda})^{-1} (\hat{\Lambda}' \hat{R}_Z(h) \hat{\Lambda}) (\hat{\Lambda}' \hat{\Lambda})^{-1}, \quad h = 1, \dots, p. \quad (29)$$

Alternatively, the estimators (29) also solve

$$\hat{\Sigma}_Y(h) = \underset{\Sigma_Y(h) \in \mathbb{R}^{r \times r}}{\operatorname{argmin}} \left\| \hat{R}_Z(h) - \hat{\Lambda} \Sigma_Y(h) \hat{\Lambda}' \right\|_F^2, \quad h = 1, \dots, p. \quad (30)$$

Having these estimators, the Yule-Walker equations can now be used to obtain the rest of the required estimators $\hat{\Psi}_1, \dots, \hat{\Psi}_p$ and $\hat{\Sigma}_\eta$. That is, $\hat{\Psi}_1, \dots, \hat{\Psi}_p$ solve the system of matrix linear equations

$$\begin{pmatrix} \hat{\Sigma}_Y(0) & \hat{\Sigma}_Y(1) & \dots & \hat{\Sigma}_Y(p-1) \\ \hat{\Sigma}_Y(1)' & \hat{\Sigma}_Y(0) & \dots & \hat{\Sigma}_Y(p-2) \\ \vdots & \vdots & \ddots & \vdots \\ \hat{\Sigma}_Y(p-1)' & \hat{\Sigma}_Y(p-2)' & \dots & \hat{\Sigma}_Y(0) \end{pmatrix} \begin{pmatrix} \hat{\Psi}_1' \\ \hat{\Psi}_2' \\ \vdots \\ \hat{\Psi}_p' \end{pmatrix} = \begin{pmatrix} \hat{\Sigma}_Y(1)' \\ \hat{\Sigma}_Y(2)' \\ \vdots \\ \hat{\Sigma}_Y(p)' \end{pmatrix} \quad (31)$$

and $\hat{\Sigma}_\eta$ is

$$\hat{\Sigma}_\eta = \hat{\Sigma}_Y(0) - \sum_{h=1}^p \hat{\Psi}_h \hat{\Sigma}_Y(h)'. \quad (32)$$

Remark 3.1 To reiterate the idea of our approach, any estimation of the latent process (PCA and Yule-Walker equations, etc.) that can be carried out on the process in terms of its second-order

properties, will have its counterpart for the considered model in terms of the observable process by using relation (14). We shall exploit this idea again in cross-validation below (Section 3.3) when selecting r and p .

3.2 Estimating link function and calculating its inverse

We assumed in Section 3.1 that link functions L_{ij} are known. In practice, they can be estimated as follows. Recall that L_{ij} is defined through marginal CDFs $F_i = F_i(\theta_i)$ and $F_j = F_j(\theta_j)$. The parameters θ_i and θ_j can then be estimated from the marginal distributions of the data $X_{i,t}$ and $X_{j,t}$, respectively. For example, an MLE can be used for most parametric CDF models of interest. The estimator \hat{L}_{ij} can be defined through the CDFs $F_i(\hat{\theta}_i)$ and $F_j(\hat{\theta}_j)$. For example, when $F_i = \text{Bern}(p_i)$, \hat{p}_i is just the sample proportion of $X_{i,t} = 1$. As another example, if the i th marginal count series follows Poisson distribution with parameter θ_i , it is estimated by the sample mean of observations, say $\hat{\theta}_i = \sum_{t=1}^T X_{i,t}/T$. Then with the computed Hermite polynomials $\hat{g}_{i,k}$ as (9), the link function for each i th and j th pair as (10) can be estimated by $\hat{L}_{ij}(u) = \sum_{k=1}^K \hat{\ell}_{ij,k} u^k$ for large enough K , say $K = 100$, on $u \in [-1, 1]$. To simplify the notation, we write L_{ij} for \hat{L}_{ij} below, and are interested in calculating L_{ij}^{-1} .

The idea to calculate L_{ij}^{-1} is as follows. Consider M -partition of the interval $[-1, 1]$ by u_0, u_1, \dots, u_M that satisfies $u_0 = -1$, $u_M = 1$, and

$$v_m := L_{ij}(u_m) \quad \text{or} \quad L_{ij}^{-1}(v_m) = u_m, \quad (33)$$

so that one has the points $(v_m, L_{ij}^{-1}(v_m)) = (v_m, u_m)$ on the curve $L_{ij}^{-1}(v) = u$. The value of $L_{ij}^{-1}(v)$ for other points v can then be obtained through some interpolation, for example, natural cubic splines (e.g. Chapter 8 in Kress, 1998). The natural cubic splines produce piecewise polynomial functions, having smooth derivatives. In addition, we use finer grids for u near ± 1 while wider grids are used around $u = 0$.

From a numerical standpoint, the $M + 1$ points (v_m, u_m) satisfy $v_m = L_{ij}(u_m)$, and the interpolation of L_{ij}^{-1} is defined as

$$\tilde{L}_{ij}^{-1}(v) =: \sum_{m=1}^M \tilde{L}_{ij,m}^{-1}(v) 1_{[v_{m-1}, v_m)}(v) \quad (34)$$

for $v \in (v_m, v_{m+1})$, $m = 0, 1, \dots, M$, with M pieces of the 3rd-order spline polynomials

$$\tilde{L}_{ij,m}^{-1}(v) = a_{m-1} \frac{(v_m - v)^3}{6h_m} + a_m \frac{(v - v_{m-1})^3}{6h_m} + b_{1,m}(v - v_{m-1}) + b_{2,m}(v_m - v), \quad (35)$$

where $h_m = v_m - v_{m-1}$. Note that v may not be divided equally. The polynomials in (35) satisfy the following constraints,

$$\tilde{L}_{ij,m}^{-1}(v_{m-1}) = u_{m-1}, \quad \tilde{L}_{ij,m}^{-1}(v_m) = u_m, \quad m = 1, \dots, M, \quad (36)$$

$$(\tilde{L}_{ij,m}^{-1})'(v_m) = (\tilde{L}_{ij,m+1}^{-1})'(v_m), \quad m = 1, \dots, M-1, \quad (37)$$

$$(\tilde{L}_{ij,m}^{-1})''(v_m) = (\tilde{L}_{ij,m+1}^{-1})''(v_m), \quad m = 1, \dots, M-1, \quad (38)$$

$$(\tilde{L}_{ij,1}^{-1})''(-v_0) = (\tilde{L}_{ij,n}^{-1})''(v_M) = 0. \quad (39)$$

Note that the knots in (36) form a continuity of the spline function. (37) and (38) ensure the second-order smoothness. (39), called the natural boundary, is required for determining polynomials uniquely. We extend the interpolation further to $[-1, 1]$ by letting $\tilde{L}_{ij}^{-1}(v) = -1$ for $v \in [-1, v_0)$ and $\tilde{L}_{ij}^{-1}(v) = 1$ for $v \in (v_M, 1]$. Since the equations (35) can be written as a symmetric tridiagonal system, it can be easily solved.

Figure 1 depicts $L_{ij}(u)$, $L_{ij}^{-1}(v)$ and its interpolation $\tilde{L}_{ij}^{-1}(v)$ for three representative marginal count distributions: Bernoulli, Poisson, and negative binomial. For example, the Bernoulli case considers a pair of $F_i = \text{Bern}(p_i)$ and $F_j = \text{Bern}(p_j)$ with four different choices of combinations (p_i, p_j) . Several combinations of parameters for other types of distributions are also considered. As seen from the plots, the inverse link function L_{ij}^{-1} obtained by flipping the axes and numerical inverse \tilde{L}_{ij}^{-1} obtained through the interpolation are nearly indistinguishable.

Remark 3.2 As noted in Section 1, we expect the estimation procedure of Sections 3.1 and 3.2 to yield consistent estimators. The recent work of Düker et al. (2023) lays the theoretical foundation for working with the model (1). As an application of their results, Düker et al. (2023) established consistency in sparse estimation of (1) when the latent process follows a sparse VAR model. The latent process here follows a factor model and the underlying model estimation is different from sparse VAR. The main result of Düker et al. (2023) can be applied to our context as well, but they rely on the assumption of concentration phenomena for the observed time series X_t having underlying VAR factor structure. We are working on proving such concentration and applying the result of Düker et al. (2023), with this work serving as a methodological and more applied study

of the model.

3.3 Selecting the number of factors and lag order of factor series

In practice, the number of factor series r and their lag order p in (4) are unknown and need to be chosen for the model estimation. We consider here several methods for this task based on available approaches, and also introduced cross-validation schemes tailored for our model. Their performance is assessed in Section 5.1.2 below, with cross-validation schemes generally outperforming others.

Selection of r : One practical approach is to examine a scree plot of the eigenvalues of $\hat{\Sigma}_Z(0) = \hat{L}^{-1}(\hat{\Sigma}_X(0))$ where the presence of a “knee” suggests the value of r . More formally, one can design an algorithm that determines the “knee.” For example, Onatski (2010) suggested the Edge Distribution (ED) estimator, whereby

$$\hat{r}(\delta) := \max\{k \leq r_{\max} : \hat{e}_k - \hat{e}_{k+1} \geq \delta\}, \quad (40)$$

where $\hat{e}_1 \geq \hat{e}_2 \geq \dots \geq \hat{e}_d$ are the ordered eigenvalues of $\hat{R}_Z(0)$ and δ is calibrated through the algorithm described in Section 4 of that paper.

Alternatively, one could rely on information criteria (IC). That is, from $q = 1, \dots, r_{\max}$, we choose the q as the estimate \hat{r} that minimizes

$$\text{IC}(q) = \ln \left(\frac{1}{dT} \|\hat{\Sigma}_\varepsilon(q)\|_F^2 \right) + qg_i(d, T), \quad (41)$$

where $\hat{\Sigma}_\varepsilon(q)$ is the estimator in (27) from the rank- q approximation of $\Sigma_Z(0)$ in (21), and $g_i(d, T) \rightarrow 0$ and $\min(d, T)g_i(d, T) \rightarrow \infty$ as $d, T \rightarrow \infty$. The recommended choices of the penalty functions $g_i(d, T)$ are

$$g_1(d, T) = \frac{d+T}{dT} \ln \left(\frac{dT}{d+T} \right), \quad (42)$$

$$g_2(d, T) = \frac{d+T}{dT} \ln(C_{dT}^2), \quad (43)$$

$$g_3(d, T) = \frac{\ln(C_{dT}^2)}{C_{dT}^2}, \quad C_{dT} = \min(\sqrt{d}, \sqrt{T}) \quad (44)$$

which corresponds to $\text{IC}_{p1}(r)$ – $\text{IC}_{p3}(r)$ studied by Bai and Ng (2002).

We now propose a block cross-validation (BCV)-based rank selection. The idea goes back at least to Browne and Cudeck (1989), and continues being utilized in psychometrics (e.g. Haslbeck

and van Bork, 2022). Differences from the setting considered here are that our observations are serially correlated and that our factor model is latent. To account for temporal dependence, we do not partition observations randomly but rather into equally sized consecutive blocks. The latent nature of the factor model will be dealt with by exploiting the idea in Remark 3.1. We thus fold $\{X_t\}$ along the time into B blocks. The superscript (b) will refer to the b th block, to be used for test data. The superscript $(-b)$ will refer to the b th block being excluded, to be used for training data. Let $\hat{R}_Z^{(b)}(0) = \hat{L}^{-1}(\hat{R}_X^{(b)}(0))$ be the sample matrix ACF of the latent Gaussian series at lag 0, computed from the sample matrix ACF of the observations from the b th block, substituted into the inverse link function. Similarly, one can compute $\hat{R}_Z^{(-b)}(0) = \hat{L}^{-1}(\hat{R}_X^{(-b)}(0))$ that excludes the b th block. Then, for each candidate rank q on a grid $q = 1, \dots, r_{\max}$, the mean square error (MSE) of BCV is defined as

$$\text{MSE}(q) = \frac{1}{B} \sum_{b=1}^B \left\| \hat{R}_Z^{(b)}(0) - \hat{R}_Z^{(-b,q)}(0) \right\|_F^2, \quad (45)$$

where $\hat{R}_Z^{(-b,q)}(0)$ is the rank- q approximation of $\hat{R}_Z^{(-b)}(0)$ plus a diagonal matrix from the estimated covariance matrix of the innovations of the factor model. The PCA-based estimation procedure described in Section 3.1 can be used. The minimizer q of the MSE is chosen as the estimate of the number of factor series r .

Instead of our PCA-based estimation, other estimation approaches can and have been used as well. For example, in the minimum residual factor analysis (MINRES, Harman and Jones, 1966), $\hat{R}_Z^{(-b,q)}(0)$ is the rank- q approximation of $\hat{R}_Z^{(-b)}(0)$ obtained by minimizing the difference between $\hat{R}_Z^{(-b)}(0)$ and the sum of $\hat{R}_Z^{(-b,q)}(0)$ and a diagonal matrix, the latter accounting for the variances of the error terms. This estimation approach is quite popular in factor analysis, with the estimation procedure implemented through R package `psych` by Revelle (2023). Other estimation approaches for factor analysis can be found in Bertsimas et al. (2017).

Selection of p : One common approach is to use the information criteria, that is,

$$\hat{p} = \underset{l}{\operatorname{argmin}} \left\{ \ln(|\hat{\Sigma}_\eta(l)|) + g_{i,l}(r, T) \right\}, \quad (46)$$

where $\hat{\Sigma}_\eta(l)$ is the estimate of the covariance matrix of the innovations of the factor series for fixed

lag order l . The possible penalty functions $g_{i,l}$ include

$$g_{1,l}(r, T) = \frac{2}{T}lr^2, \quad (47)$$

$$g_{2,l}(r, T) = \frac{2 \log(\log(T))}{T}lr^2, \quad (48)$$

$$g_{3,l}(r, T) = \frac{\log(T)}{T}lr^2, \quad (49)$$

$$g_{4,l}(r, T) = \frac{2r(rl + 1)}{T}. \quad (50)$$

The resulting criteria can be found in Chapter 4.3 of Lütkepohl (2005).

We now propose a cross-validation strategy tailored to our model. We shall exploit once again the idea of Remark 3.1. Were the factor series Y_t observed, a natural cross-validation scheme would select p as l minimizing

$$\sum_{b=1}^B \sum_t \left\| Y_t^{(b)} - \hat{\Psi}_1^{(-b)} Y_{t-1}^{(b)} - \dots - \hat{\Psi}_l^{(-b)} Y_{t-l}^{(b)} \right\|_F^2, \quad (51)$$

where $\hat{\phi}_h^{(-b)}$ are the VAR transition matrices estimated on the training data, and $Y_t^{(b)}$ refer to the testing data. Setting

$$\mathcal{Y}^{(b,l)} = (Y_t^{(b)})'_t, \quad \hat{\Psi}^{(-b,l)} = \begin{pmatrix} \hat{\Psi}_1^{(-b)'} \\ \vdots \\ \hat{\Psi}_l^{(-b)'} \end{pmatrix}, \quad \mathcal{X}^{(b,l)} = \begin{pmatrix} Y_{t-1}^{(b)'} & \dots & Y_{t-l}^{(b)'} \end{pmatrix}_t, \quad (52)$$

the function to minimize can be replaced by

$$\sum_{b=1}^B \left\| \mathcal{Y}^{(b,l)} - \mathcal{X}^{(b,l)} \hat{\Psi}^{(-b,l)} \right\|_F^2 = \sum_{b=1}^B \text{vec} \left(\mathcal{Y}^{(b,l)} - \mathcal{X}^{(b,l)} \hat{\Psi}^{(-b,l)} \right)' \text{vec} \left(\mathcal{Y}^{(b,l)} - \mathcal{X}^{(b,l)} \hat{\Psi}^{(-b,l)} \right) \quad (53)$$

or

$$\sum_{b=1}^B \left(-2 \hat{\psi}^{(-b,l)'} \hat{\gamma}_Y^{(b,l)} + \hat{\psi}^{(-b,l)'} \hat{\Gamma}_Y^{(b,l)} \hat{\psi}^{(-b,l)} \right), \quad (54)$$

where $\hat{\psi}^{(-b,l)} = \text{vec}(\hat{\Psi}^{(-b,l)})$ and

$$\hat{\gamma}_Y^{(b,l)} = \text{vec}(\mathcal{X}^{(b,l)'} \mathcal{Y}^{(b,l)}), \quad \hat{\Gamma}_Y^{(b,l)} = I_r \otimes \mathcal{X}^{(b,l)'} \mathcal{X}^{(b,l)}. \quad (55)$$

Following the idea of Remark 3.1, note that the quantities in (55) are obtained from the (sample)

second-order properties of $(Y_t^{(b)})$. For our model, they can be replaced by those implied by the equation (14) based on the observed data $(X_t^{(b)})$. Similarly, we already have the estimators $\hat{\Psi}^{(-b,l)}$ calculated from the observed data $(X_t^{(-b)})$. In summary, as a cross-validation scheme to select p for our model, we also minimize (54) but where the quantities involved are computed on the training data $(X_t^{(-b)})$ and the testing data $(X_t^{(b)})$.

Remark 3.3 Note that determining the number of factors can be performed regardless of the lag order of the factor series. We thus recommend choosing \hat{r} first, followed by selecting \hat{p} .

4 Forecasting

4.1 Particle-based sampling procedure

A fitted latent Gaussian dynamic factor model in (1)–(4) can naturally be used to forecast the series X_t . We will show how this can be carried out for fixed model parameters. For example, the model parameters can be obtained through estimation (in which case our forecast will not reflect any uncertainty from estimation error). More specifically, for a given t (typically, $t = T$, the sample length), we are interested in the distribution of

$$\hat{X}_{t+h|t} = (X_{t+h}|X_1 = x_1, \dots, X_t = x_t), \quad (56)$$

where $h = 1, 2, \dots$, the vertical bar indicates the conditioning and x_1, \dots, x_t are the observed values of X_1, \dots, X_t . This is equivalent to finding

$$\mathbb{E}_{x_{1:t}} \left[V(\hat{X}_{t+h|t}) \right] \quad (57)$$

for arbitrary function V , where the subscript $x_{1:t}$ in $\mathbb{E}_{x_{1:t}}$ refers to the conditioning on $\{x_1, \dots, x_t\}$ as in (56). For example, suppose we have a d –dimensional vector x . With $V(x) = V((x_i)_{i=1,\dots,d}) = 1_{\{x_i=n_i, i=1,\dots,d\}}$ and d –dimensional integer n , the quantity (57) becomes $\mathbb{P}_{x_{1:t}}(\hat{X}_{t+h|t} = n)$, which is of primary interest in forecasting X_{t+h} , when the components of X_t are integer-valued.

Let $\hat{Z}_{t+h|t} = \hat{Z}_{t+h}(Z_{1:t}) = H_{t1}^{(h)} Z_t + \dots + H_{tt}^{(h)} Z_1$ be the h –step-ahead linear prediction of Z_{t+h} from $Z_{1:t}$. Define $\hat{R}_{t+h|t} = \mathbb{E}[(Z_{t+h} - \hat{Z}_{t+h|t})(Z_{t+h} - \hat{Z}_{t+h|t})']$ as the corresponding covariance matrix of prediction error of Z_{t+h} . One can compute the latent prediction $\hat{Z}_{t+h|t}$ by using Kalman recursions as recalled in Appendix A. This exploits the state-space structure of the model and is

more efficient computationally than a direct application of e.g. Durbin-Levinson algorithm. Then, the quantity (57) can be expressed as

$$\mathbb{E}_{x_{1:t}} \left[V(\hat{X}_{t+h|t}) \right] = \mathbb{E}_{x_{1:t}} \left[D_{V,t+h}(\hat{Z}_{t+h|t}) \right], \quad (58)$$

where

$$D_{V,t+h}(z) = \int_{\mathbb{R}^d} V(G(z_{t+h})) \frac{\exp \left(-\frac{1}{2} (z - z_{t+h})' \hat{R}_{t+h|t}^{-1} (z - z_{t+h}) \right)}{(2\pi)^{d/2} |\hat{R}_{t+h|t}|^{1/2}} dz_{t+h} \quad (59)$$

(see equations (23)–(24) in Jia et al., 2023). The right-hand side of (58) will be approximated through a Monte Carlo scheme below; direct numerical calculation of underlying integrals is too cumbersome.

Note that conditioning on $x_{1:t}$ does not determine the exact path of $z_{1:t}$. Indeed, recall from (2) that for $j = 1, \dots, d$,

$$\{X_{j,t} = x_{j,t}\} = \{\Phi^{-1}(C_{j,x_{j,t-1}}) < Z_{j,t} \leq \Phi^{-1}(C_{j,x_{j,t}})\} = \{Z_{j,t} \in A_{j,x_{j,t}}\}, \quad (60)$$

where $C_{j,m} = \mathbb{P}(X_{j,t} \leq m)$ and $A_{j,x_j} = (\Phi^{-1}(C_{j,x_{j-1}}), \Phi^{-1}(C_{j,x_j})]$. That is, each entry of the realization of X_t is determined by the range of the corresponding entry of Z_t at each time t . For d -dimensional observations, one has

$$\{X_t = x_t\} = \bigcap_{j=1}^d \{Z_{j,t} \in A_{j,x_{j,t}}\} = \{Z_t \in A_{x_t}\}, \quad (61)$$

where $A_{x_t} = A_{1,x_{1,t}} \times \dots \times A_{d,x_{d,t}}$. The notation A_{j,x_j} and A_x will be used below. In the Bernoulli case, for example,

$$A_{j,x_{j,t}} = (\Phi^{-1}(C_{j,x_{j,t-1}}), \Phi^{-1}(C_{j,x_{j,t}})] = \begin{cases} (\Phi^{-1}(1 - p_j), \infty), & \text{if } x_{j,t} = 1, \\ (-\infty, \Phi^{-1}(1 - p_j)], & \text{if } x_{j,t} = 0. \end{cases} \quad (62)$$

The Bernoulli marginal distribution thus has the largest ranges for Z_t . In a Monte Carlo approximation of (58), one will be generating $Z_{j,t} \in A_{j,x_{j,t}}$ and producing their forecast $\hat{Z}_{j,t+h}$.

The following presentation extends that of Jia et al. (2023) to the multivariate setting relevant to the Monte Carlo approximation problem. The quantity (58) is known to be well approximated through Sequential Monte Carlo (SMC) by generating “particles” over time t (e.g. Doucet et al., 2001, Doucet and Johansen, 2009). The main difference from Jia et al. (2023) is that the model

here has two latent processes $\{Z_t\}$ and $\{Y_t\}$. To deal with the two latent processes, we use Kalman recursions to forecast and update the latent process $\{Y_t\}$ and approximate the distribution of $\{Z_t\}$ conditioning on $\{X_t\}$. This approach is called Rao-Blackwellization and the method is adapted from the partially observed Gaussian state-space models (e.g. Andrieu and Doucet, 2002, Briers et al., 2010).

The following is the SMC algorithm for particle filtering to generate particles $\{\tilde{Z}_t^{(k)}\}_{t=1,\dots,T}$, $k = 1, \dots, N$, over time, whose weighted average then approximates (58). The particle $\{\tilde{Z}_t^{(k)}\}$ can be regarded as the realization of the underlying latent process. Additionally, we add a resampling step which is often used in sequential Monte Carlo algorithms. We will explain the necessity of resampling below.

Sequential Importance Sampling and Resampling (SIS/R): Set the initial importance weights $w_0^{(k)} = 1$ for all k , initialize $\tilde{Y}_{0|0}^{(k)} \sim \mathcal{N}(0, \tilde{Q}_{0|0})$, where $\tilde{Q}_{0|0} = \text{Var}(Y_0)$. For $p = 1$, $\tilde{Q}_{0|0}$ is approximated by $\sum_{m=0}^M \Psi^m \Sigma_\eta (\Psi')^m$ for large M . Then, recursively over $t = 1, \dots, T$, do the following steps: For each $k = 1, \dots, N$:

1. Forecasting step: Compute $\hat{Y}_{t|t-1}^{(k)}$, $\hat{Q}_{t|t-1}$, $\hat{Z}_{t|t-1}^{(k)}$ and $\hat{R}_{t|t-1}$ via Kalman recursions (see Appendix A).
2. Importance sampling step: Sample residual $\xi_t^{(k)}$ satisfying

$$\xi_t^{(k)} \stackrel{d}{=} \mathcal{N}_d \left(0_d, I_d \middle| \Phi^{-1}(C_{x_{t-1}}) < \hat{Z}_{t|t-1}^{(k)} + \hat{R}_{t|t-1}^{1/2} \xi_t^{(k)} \leq \Phi^{-1}(C_{x_t}) \right), \quad (63)$$

where $\Phi^{-1}(C_n) = (\Phi^{-1}(C_{1,n_1}), \dots, \Phi^{-1}(C_{d,n_d}))'$ and $\mathcal{N}_d(\mu, \Sigma|A)$ indicates a d -dimensional multivariate normal distribution with mean μ and covariance Σ restricted to the set A . Then, update the particle as

$$\hat{Z}_t^{(k)} = \hat{Z}_{t|t-1}^{(k)} + \hat{R}_{t|t-1}^{1/2} \xi_t^{(k)} \quad (64)$$

and update the importance weight as $w_t^{(k)} = w_{t-1}^{(k)} w_t(\hat{Z}_{t|t-1}^{(k)})$, where

$$w_t(\hat{Z}_{t|t-1}^{(k)}) = \mathbb{P} \left(\mathcal{N}(\hat{Z}_{t|t-1}^{(k)}, \hat{R}_{t|t-1}) \in A_{x_t} \right). \quad (65)$$

3. Resampling step: Set $\Omega_{t,N} = \sum_{k=1}^N w_t^{(k)}$ and normalize $w_t^{(k)}$ by $\tilde{w}_t^{(k)} = w_t^{(k)} / \Omega_{t,N}$. Take a quartet $(\tilde{w}_t^{(k)}, \tilde{Y}_{t|t-1}^{(k)}, \tilde{Z}_{t|t-1}^{(k)}, \tilde{Z}_t^{(k)})$ as follows.

- If a resampling criterion described around (67) is satisfied, then take $(\frac{1}{N}, \hat{Y}_{t|t-1}^{(I_k)}, \hat{Z}_{t|t-1}^{(I_k)}, \hat{Z}_t^{(I_k)})$,

where $\{I_k\}$ are chosen indices after resampling.

- If the criterion is not satisfied, then take $(\tilde{w}_t^{(k)}, \hat{Y}_{t|t-1}^{(k)}, \hat{Z}_{t|t-1}^{(k)}, \hat{Z}_t^{(k)})$.

4. Updating step: Use $\tilde{Y}_{t|t-1}^{(k)}, \tilde{Z}_{t|t-1}^{(k)}, \tilde{Z}_t^{(k)}$ and $\hat{Q}_{t|t-1}$ to compute $\tilde{Y}_{t|t}^{(k)}$ and $\tilde{Q}_{t|t}$ via Kalman recursions (see Appendix A).

Finally, the SMC approximation of (58) becomes

$$\mathbb{E}_{x_{1:t}}[V(\hat{X}_{t+h|t})] \approx \sum_{k=1}^N \tilde{w}_t^{(k)} D_{V,t+h}(\hat{Z}_{t+h|t}^{(k)}), \quad (66)$$

where $\hat{Z}_{t+h|t}$, $h \geq 1$, are computed through forecasting step in the Kalman recursions. See equation (25) in Jia et al. (2023) for the justification of an analogous approximation.

The SMC is known to suffer from the so-called weight degeneracy of particles (e.g. Snyder et al., 2008) which occurs when the variance of normalized weights becomes inflated. The latter happens and becomes worse as the sample size increases. To overcome this, it is suggested to remove the particles with small weights. By following Doucet and Johansen (2009), we resample only when the effective sample size (ESS) exceeds $N/2$, as a rule of thumb, for the criteria of resampling, where the ESS is defined as

$$\text{ESS}_t = \left(\sum_{k=1}^N \left(\tilde{w}_t^{(k)} \right)^2 \right)^{-1}. \quad (67)$$

More specifically, we resample particles by following systematic resampling. That is, sample $U_1 \sim \mathcal{U}(0, 1/N)$ and set $U_k = U_1 + \frac{k-1}{N}$, $k = 2, \dots, N$. Then, compute

$$I_k = \left| \left\{ U_i : \sum_{j=1}^{k-1} \tilde{w}_t^{(j)} \leq U_i \leq \sum_{j=1}^k \tilde{w}_t^{(j)} \right\} \right| \quad (68)$$

with $\sum_{j=1}^0 = 0$ as a convention. This is used in Step 3 of the SIS/R algorithm above. Alternatively, one can use multinomial resampling, which is resampling particles by regarding $\{\tilde{w}_t^{(k)}\}$ as a multinomial probability distribution. Many other resampling methods exist (see Douc and Cappé (2005) for more information).

Remark 4.1 The forecasting distribution (57) is characterized by the function $V(x) = V((x_i)_{i=1,\dots,d}) = 1_{\{x_i=n_i, i=1,\dots,d\}}$ for fixed $n = (n_i)_{i=1,\dots,d}$. For a single d -dimensional forecast value, one could take $n = (n_i)_{i=1,\dots,d}$ for which (57) is largest with the corresponding functions $V(x)$. Note, however, that this is a daunting task computationally. For example, even with the Bernoulli marginals where

$n_i = 0$ or 1 , the number of functions V to consider is 2^d , which grows exponentially in d . To sidestep this issue, we only consider $V(x) = 1_{\{x_i=n_i\}}$ in practice and take n_i as the forecast value in the i th coordinate for which (57) is largest. E.g. in the Bernoulli case, this task computationally is of the order d .

4.2 Speed-up in forecasting computation

The computation burden for sequential Monte Carlo sampling is substantial. The majority of the cost is due to sampling (doubly) truncated multivariate Gaussian random variables $\{\xi_t^{(k)}\}$ in (63), and the fact that the algorithm runs for $t = 1, \dots, T$. Currently, we implement sampling through the R package `tmvtnorm` developed by Wilhelm and Manjunath (2010). But an improvement in the computation speed for generating truncated multivariate normal random variables is not expected.

To reduce the computational cost, we note that the covariance matrices $\hat{R}_{t|t-1}$ of prediction error typically converge within a few steps. This is due to a similarly quick convergence of the covariance matrix $\hat{Q}_{t|t-1}$ of prediction error of the factor series in (83), and the covariance matrix $\tilde{Q}_{t|t}$ and Kalman gain K_t described in (86).

From the pair of covariance matrices in (83) and (86), one has the recursive equation

$$\hat{Q}_{t+1|t} = \Psi \left(\hat{Q}_{t|t-1} - \hat{Q}_{t|t-1} \Lambda' (\Lambda \hat{Q}_{t|t-1} \Lambda' + \Sigma_\varepsilon)^{-1} \Lambda \hat{Q}_{t|t-1} \right) \Psi' + \Sigma_\eta, \quad (69)$$

with the given initial condition $\hat{Q}_{1|0} = \Psi \tilde{Q}_{0|0}$. The covariance matrices of the prediction error converge to a positive definite matrix Q satisfying the discrete algebraic Riccati equation (DARE),

$$Q = \Psi \left(Q - Q \Lambda' (\Lambda Q \Lambda' + \Sigma_\varepsilon)^{-1} \Lambda Q \right) \Psi' + \Sigma_\eta. \quad (70)$$

One has a similar equation for the covariance matrices $\tilde{Q}_{t|t}$. It is the convergence to these equations that happens within a few time steps substantially shorter than the length of observations T . Since the purpose of the SIS/R algorithm is to obtain the importance weights $\{\tilde{w}_T^{(k)}\}$ along the particles $\{Z_{1:T}^{(k)}\}$ and we presume the stable factor series, it is reasonable to run the forecasting algorithm with only a few last observations. In simulation and application below, we employ the forecasting algorithm with the last 10 observations.

4.3 On forecasting for longer horizons

In this section, we briefly discuss what to expect from the forecasting method when the forecasting horizon h becomes longer. Recall that the latent factor series is stationary and follows a stable VAR model. The latent process $\{Z_t\}$ is also stationary and its long-term prediction converges to its mean, which is a zero vector. From (94) and (96), the predicted particles are therefore expected to converge eventually to zero vectors as well. Thus, for longer horizon h , we expect

$$\mathbb{E}_{x_{1:t}}[V(\hat{X}_{t+h|t})] \approx D_{V,t+h}(0). \quad (71)$$

As in Remark 4.1, consider $V(x) = V(x_i) = 1_{\{x_i=n_i\}}$, $i = 1, \dots, d$. For $\hat{Z}_{t+h|t} = z = 0$, (59) becomes

$$\begin{aligned} D_{V,t+h}(0) &= \int_{\mathbb{R}^d} 1_{\{(G(z_{t+h}))_i=n_i\}} \frac{\exp\left(-\frac{1}{2}(z_{t+h})' \hat{R}_{t+h|t}^{-1}(z_{t+h})\right)}{(2\pi)^{d/2} |\hat{R}_{t+h|t}|^{1/2}} dz_{t+h} \\ &= \int_{\{G_i(z_{i,t+h})=n_i\}} \frac{\exp\left(-\frac{1}{2}z_{i,t+h}^2/(\hat{R}_{t+h|t})_{ii}\right)}{\sqrt{2\pi} |(\hat{R}_{t+h|t})_{ii}|^{1/2}} dz_{i,t+h}, \end{aligned} \quad (72)$$

where $(\hat{R}_{t+h|t})_{ii}$ is the i th diagonal entries of covariance matrix $\hat{R}_{t+h|t}$. For longer horizon h , $(R_{t+h|t})_{ii} \approx \text{Var}(Z_{i,t}) = 1$. We thus expect from (71) and (72) that for longer horizon h ,

$$\mathbb{E}_{x_{1:t}}[1_{\{(\hat{X}_{t+h|t})_i=n_i\}}] \approx D_{V,t+h}(0) \approx \mathbb{P}(Z \in A_{i,n_i}) = \mathbb{P}(X_i = n_i), \quad (73)$$

where $Z \sim \mathcal{N}(0, 1)$ and X_i has a CDF F_i with the parameter θ_i . Hence, for longer horizon h , our forecasting method can be thought as choosing n_i among possible values that maximizes the most likely count value according to the distribution F_i with the parameter θ_i . Two observations are worth making in this regard.

First, in some instances, e.g. Bernoulli and multinomial distributions, θ_i represents proportion of count values and is estimated as the corresponding sample proportions. In these cases, for long horizon h , we therefore expect our forecast to yield the most likely observed count (modulo the issue of ties). This is the case with the application considered in Section 6. On the other hand, for many other distributions, this observation may not necessarily hold. For example, for the Poisson distribution, the parameter is taken as the sample mean and the most likely count according to this Poisson distribution does not need to be the most likely value, let alone be in the sample.

Second, the relation (73) might be confusing from the following point of view. As argued above,

for longer horizon h , we expect $\hat{Z}_{t+h|t} \approx 0$. In fact, we see this clearly in the application of Section 6. The relation (73) might be read as saying that 0 belongs to the bin A_{i,n_i} with the highest standard normal probability. This is, however, not necessarily the case. It will be the case when n_i is the median of the distribution F_i (i.e. $F_i(n_i - 1) < 1/2$ and $F_i(n_i) \geq 1/2$), a quite likely scenario in practice especially for “bell-shaped” distribution with the most likely value n_i being at the center, but the statement will not hold in general.

5 Simulation study

In this section, we assess the performance of estimation and forecasting procedures introduced in Sections 3 and 4. Here, we focus on Bernoulli, Poisson, and negative binomial marginal distributions with several parameter values.

5.1 Estimation

5.1.1 Model parameter estimation for known number of factors and lag order

The model setting in the simulation is defined as follows. For the order p of factor series $\{Y_t\}$ in (4), we take $p = 1$ and it is assumed to be given. The dimension is either $r = 2$ or $r = 5$, which is assumed to be known as well. The corresponding transition matrices $\Psi = (\psi_{ij})$ are diagonal for simplicity but all the entries are either 0.7 (positive correlation) or -0.7 (negative correlation). The corresponding matrices are denoted $\Psi_1^{(1)}$ and $\Psi_1^{(2)}$, respectively. We consider $\Sigma_\eta = I_r$ and $\Sigma_\varepsilon = I_d$. Following (24), the component Λ_2 of the loadings matrix Λ in (3) is generated as follows. The entries $\lambda_{i,j}$, $i = 1, \dots, d - r$, $j = 1, \dots, r$, in Λ_2 are independently drawn from the uniform distribution $U(0, 1)$. We consider the same parameters $\{\theta_i\}$ and marginal count distributions as for the illustrative examples of link functions in Figure 1. For Bernoulli case, d component series are divided into 3 equal groups having $\theta_i = p_i = 0.2, 0.4, 0.7$, respectively. Similarly, for Poisson marginal counts with $\theta_i = \lambda_i = 0.1, 1$, and 10, and for negative binomial case with $\theta_i = p_i = 0.2, 0.4, 0.7$ and the number of successes 3. Monte Carlo simulations are based on 100 replications for each setting.

The performance of our estimators is assessed through relative ℓ_2 losses, which are defined as

$$L(\hat{a}) = \frac{\mathbb{E}\|\hat{a} - a\|_F}{\|a\|_F}, \quad (74)$$

where \hat{a} is an estimator of the parameter a . The reported losses are computed as averages over 100 replications. The numerical biases of our estimators are defined as

$$B(\hat{a}) = \frac{\|\mathbb{E}[\hat{a}] - a\|_1}{\|a\|_1}, \quad (75)$$

where \hat{a} is an estimator of the parameter a . Similar to the relative ℓ_2 losses, the reported bias is computed as averages over 100 replications.

Table 1 summarizes the estimation results for several d and T values. Generally, the results are as expected. For example, both the losses and the biases decrease with increasing sample size T . As the dimension d increases, both the losses and the biases decrease as well. When the number of factors gets larger, then the corresponding losses and biases increase. Additionally, when the transition matrix $\Psi_1^{(2)}$ of VAR has negative entries the losses and the biases are diminished compared to those for $\Psi_1^{(1)}$.

Another interesting point is that the estimation losses for the underlying factor series $(\hat{\Psi}, \hat{\Sigma}_\eta)$ are larger than the losses from the factor model $(\hat{\Lambda}, \hat{\Sigma}_\varepsilon)$. In terms of biases, the values concerning the covariance matrix of factor series are not larger than those from the covariance matrix of factor models. However, when considering the number of entries in parameters, the contribution of each estimate is relatively large in the factor series compared to that from the factor model. The factor series parameters are estimated using factor model constructs so that estimation is naturally more difficult. Furthermore, the differences in estimation losses between the different marginal count distributions are not substantial.

5.1.2 Selection of the number of factors and lag order

We illustrate the performance of the selection of the number of factors r and the lag order p , suggested in Section 3.3. The exact same model parameters as in Section 5.1.1 are used in the context of finding the number of factor series. We denote the scree plot method of finding the “knee” described in (40) by ED. The IC methods as combinations of (41) with the three different penalty functions (42)–(44) are denoted by IC1–IC3, respectively. For the BCV-based approach, we employ two different estimation procedures. Our principle component-based estimation in Section 3.1 is denoted by BCV(PC). On the other hand, BCV(FAC) refers to MINRES estimation by Harman and Jones (1966), which is briefly described in Section 3.3. For each combination of model parameters, 100 replications are performed.

For selecting the lag order of factor series, we additionally introduce two sets of VAR transition matrices $\Psi^{(3)} = \{\Psi_1^{(3)}, \Psi_2^{(3)}\}$ and $\Psi^{(4)} = \{\Psi_1^{(4)}, \Psi_2^{(4)}, \Psi_3^{(4)}, \Psi_4^{(4)}\}$. Those two sets of parameters are used to produce factor series Y_t governed by VAR(2) and VAR(4), respectively. The diagonal entries of the transition matrices are

$$(\psi_{ii,1}^{(3)}, \psi_{ii,2}^{(3)}) = (0.7, -0.4), \quad (76)$$

$$(\psi_{ii,1}^{(4)}, \psi_{ii,2}^{(4)}, \psi_{ii,3}^{(4)}, \psi_{ii,4}^{(4)}) = (0.7, -0.2, 0.3, -0.4), \quad (77)$$

and the off-diagonal entries are zero otherwise. These choices of the true lag orders will be denoted by $p = 2$ and $p = 4$ in the presented results, respectively. The rest of the parameters and the size of the problems remain the same as in other simulations. For baselines, the IC methods in (46) are considered combined with the four penalties (47)–(50) as Akaike information criterion (AIC), Hannan-Quinn criterion (HQ), Bayesian arguments Schwarz criterion (SC), and final prediction error criterion (FPE), respectively. 100 replications are performed per each combination of parameters.

The selection results are depicted in Figures 2 and 3 as the frequencies of estimated r and p in 100 replications. In Figure 2, the BCV(PC) method outperforms all baselines (ED, IC1–3) in selecting true r , followed by BCV(FAC). The quality of estimation by the BCV-based approaches follows the pattern in the estimation of model parameters. That is, as the dimension d and sample length T increase, so do the percentages of correctly estimated r . In terms of marginal distributions, BCV(PC) works best for negative binomial, but the other two distributions are not that behind. Interestingly, BCV(FAC) tends to overestimate for some cases, especially when the true number of factor series is large, $r = 5$ in our simulation.

Turning to Figure 3, determining the lag order p seems more difficult. Whereas the non-BCV-based baselines for r in the previous experiments tended to be more correct as either d or T increased, the IC methods now perform poorly for all conditions. Even for the BCV approach, the results are mixed. When the number of factor series is small, $r = 2$, the correct lag orders tend to be estimated in the majority of replications. The estimation performance degrades considerably for a large number of factor series, $r = 5$. The results improve for larger sample length ($T = 400$) and are best for the negative binomial distribution. A more accurate lag order selection procedure, however, would still be desirable.

5.2 Forecasting

In this section, we assess forecasting performance in the simulation setting considered in Section 5.1.1. We generate h -step-ahead prediction $V(\hat{X}_{T+h|T})$ through (66). The importance weights $\{\hat{w}_T^{(k)}\}$ are calculated through the SIS/R algorithm. The generation of h -step-ahead prediction $\hat{Z}_{T+h|T}$ is described in Appendix A.

We hold out the last 5 observations and use $T - 5$ observations as given. Within the latter sample, the model is fitted and the last 10 observations are used for estimating covariances $\hat{Q}_{t|t-1}$, $\hat{Q}_{t|t}$, and Kalman gain K_t as discussed in Section 4.2. The rest of prediction follows the Kalman recursions as discussed in Appendix A.

The performance is evaluated by the following three measures. The first three measures are related to the Gaussian latent process and its transformation through the marginal distribution. For the Gaussian process, it is worth measuring the total error due to the difference between $\{\hat{Z}_{T+h|T}^{(k)}\}_{k=1,\dots,N}$ and Z_{T+h} caused by particles since the correctly produced $\hat{Z}_{T+h|T}^{(k)}$ leads to the higher likelihood that the latent process lies in the bin that produces the observation identical to the observation X_{T+h} . Besides, each particle contributes to forecasting X_{T+h} so the more particles deviate from the truth, the more variability the forecasted values should take. Likewise, we can compute the forecasts of the latent factor series $\hat{Y}_{T+h|T}^{(k)}$ and consider the difference from Y_{T+h} . Also, we compute the root mean forecasting error of $X_{T+h|T}$ over the average of 100 realized particles in forecasting window. Specifically, the root mean h -step forecasting errors of the latent processes and the observation process for one replication (realization) are computed as

$$RMFE_Y(h) = \sqrt{\frac{\frac{1}{N} \sum_{k=1}^N \sum_{i=1}^r (\hat{Y}_{i,T+h|T}^{(k)} - Y_{i,T+h})^2}{\frac{1}{T} \sum_{i=1}^r \sum_{t=1}^T Y_{i,t}^2}}, \quad h = 1, 2, \dots, H, \quad (78)$$

$$RMFE_Z(h) = \sqrt{\frac{\frac{1}{N} \sum_{k=1}^N \sum_{i=1}^d (\hat{Z}_{i,T+h|T}^{(k)} - Z_{i,T+h})^2}{\frac{1}{T} \sum_{i=1}^d \sum_{t=1}^T Z_{i,t}^2}}, \quad h = 1, 2, \dots, H, \quad (79)$$

$$RMFE_X(h) = \sqrt{\frac{\sum_{i=1}^d (\hat{X}_{i,T+h|T} - X_{i,T+h})^2}{\frac{1}{T} \sum_{i=1}^d \sum_{t=1}^T X_{i,t}^2}}, \quad h = 1, 2, \dots, H. \quad (80)$$

Finally, we report the sensitivity defined as

$$Sens(h) = \frac{1}{d} \sum_{i=1}^d 1_{\{\hat{X}_{i,T+h|T} = X_{i,T+h}\}}, \quad h = 1, 2, \dots, H. \quad (81)$$

Each Monte Carlo simulation is based on 100 replications and the averages are reported. Note that this measure is stringent, in that it reports the matching rate entrywise. In addition, we consider two baselines. First, as the most naive forecasting method, we use the last observation. We call this Last observation (denoted Last or L). Second, we consider each dimension $i = 1, \dots, d$ separately and define the predictions as the likeliest previous value for that dimension. For example, if the most frequent value $X_{1,t}$ for the first dimension $i = 1$ within the observation window is 3 for the Poisson case, we take 3 as predictions for all 5 steps ahead. We call this approach Marginal likelihood (denoted Marginal or M); see also Section 4.3. The forecasting accuracy of those two baselines is measured by sensitivity.

Table 2 reports the results. In general, square-root forecasting errors of both the observations X_t and the two latent processes Z_t and Y_t gradually increase with the longer forecasting horizon. The difference between the forecasting errors of the observation and latent process is that the increasing trend for $RMFE_Z$ and $RMFE_Y$ along the forecasting horizon h seems more pronounced. The forecasting error of factor series is also larger than the observation series. Furthermore, it is interesting that the forecasting error of the factor series depends on the dimension d rather than the number of factors r , with the error decreasing as d increases. The sensitivity, on the other hand, seems to exhibit similar performance along the horizon, with the longer horizon outperforming for some cases. Perhaps as expected, the sensitivity of our method has scored better than both Last and Marginal approaches for all combinations of simulations. Among different marginal distributions, Bernoulli cases have the best performance followed by the Poisson in terms of sensitivity. The negative binomial cases have the lowest sensitivity scores, but the difference in $RMSFE_X$ from the Poisson cases is relatively small. Interestingly, the $RMSFE_Z$ s and $RMSFE_Y$ s among the 3 different distributions are similar. Furthermore, forecasting performances for the different numbers of factors are also similar. However, a significant difference in performance has been found for different dimensions d . A significant difference in performance has also been found in the different transition matrix cases, with better forecasting in the case of negative dependence ($\Psi_1^{(2)}$). This is intuitive in that the fluctuations of the latent process around the bin thresholds happen more frequently across the temporal series.

6 Application

To demonstrate the utility of the proposed model, we consider individual-level time series consisting of daily self-report measures of personality collected by Borkenau and Ostendorf (1998). That study was designed to explore items describing personal emotions representing the “Big Five” factors of personality. The structure of the data is as follows. 30 items of emotions where groups of 6 items are known to be related to one of the five factors in personality have been collected for 22 students over 90 days.

All 30 items are thought to correspond to at least one of the “Big Five” factors. These categories are known to follow a factor structure, and are denoted as categories 1 through 5 below. Each evening the participants of the study were instructed to appraise their daily behavior for each item on a scale ranging from 0 to 6, with 6 indicating greater endorsement of the emotion that day. For illustrative purposes, we work with the data for one student out of the 22 available. The choice of the student was largely motivated by the following consideration: for many students, response on some items showed very little variability (i.e., being mostly constant) and such cases were not particularly interesting from the time series perspective. We reduce the effect of the two extreme observations 0 and 6 by merging them with 1 and 5, respectively, so that the new scale ranges from 1 to 5. The practitioners wishing to use our (or any other) model should first carry out some basic explanatory analysis of data, as we touch upon below.

The data set and its time series plots are illustrated in Figure 4. Among 90 consecutive observations, we use the first 85 observations for estimation and the last 5 observations as a hold-out sample to evaluate our forecasts. The corresponding 6 items are grouped by the identified categories C1 through C5. The time series of individual items show substantial variability. We also see from the time plots that the dynamics of the 6 items in each category share common features. Hence, it is plausible to postulate the existence of a latent factor structure that drives the dynamics.

The following remarks provide further evidence for the latent factor structure. Several estimated correlation matrices are depicted in Figure 5. The top panel presents the sample autocorrelation matrices of the observed series X_t . The bottom panel presents the estimated autocorrelation matrices of the latent series Z_t . For both panels, the left plot is for lag 0 and the right plot is for lag 1. One can see that both autocorrelation matrices for the same lag order are nearly indistinguishable. At lag 0, the plots in both panels show clear block patterns characteristic of the factor structure. Furthermore, the factor structure seems to be preserved through temporal

dependence as suggested by the plots of the sample ACFs at lag 1, though it is less discernible.

The BCV methods for the number of factors in Section 3.3 also select $r = 5$. The BCV method for the lag order in Section 3.3 suggests $p = 1$. We thus work with the model assuming $r = 5$, $p = 1$. For these selections and in the estimation results below, we assume multinomial distributions on $\{1, 2, 3, 4, 5\}$ as marginal distributions. Now R Figure 6 presents the estimated loading matrix and Figure 7 depicts the transition matrix of the factor series estimated through the method described in Section 3. This pattern is consistent with what we observe in Figure 5. Note that the transition matrix has relatively large values not only on the diagonal but also for some off-diagonal entries. The large off-diagonal values indicate that there are cross-correlations across the factor series.

With the estimated model, we forecast the next 5 steps as discussed in Remark 4.1 and compare the values with the true ones held out of the sample. For comparison, we consider two simple forecasting approaches, Last and Marginal, as described in Section 5.2.

Figures 8 and 9 present the generated particles $\{\hat{Z}_t^{(k)}\}$ for 30 items within the last 10 observations and the predicted values of latent process $\{\hat{Z}_{T+h|T}^{(k)}\}$ for next 5 forecasting steps, respectively. The items have been grouped using the 5 underlying categories. The three or four parallel lines in Figures 8 and 9 represent the thresholds, and each pair of lines represents a bin. To distinguish the values, we use different line types for each threshold. As explained above, the particles are generated at each time point to belong to a certain bin that matches the discrete observation for that dimension. This is why the particles stay within bins at all time points in the left panel. For some of the items, a thresholding line is placed outside the given vertical scale. This is due to the way the bins are defined. Note that since each bin is estimated through the observations, some values do not appear if they are not realized in the observation period. Those values are also excluded from the candidate forecasting values. On the other hand, since no further observations are assumed to be given after the observation period, the particles are generated by forecasting the latent process. For this reason, the particles in the right panel do not need to stay in the same bin. Note that all of the particles seem to converge to zero for the longer forecasting horizon. As explained in Section 4.3, this is natural when a stable VAR is used for forecasting. Note also that the particles are rather close to zero even for the first few horizons. This is a consequence of the interplay between the levels of signal (factors) and noise (errors) in the estimated model. The forecasted value naturally takes 0 when forecasting noise and thus downweights the factor forecast as the larger the noise magnitude is, since the variance of our latent process is 1 in each dimension.

Finally, Figure 10 shows the plots of the absolute differences between forecasts and the true

values for each item. The items are ordered to match the categories expecting that each factor mainly affects the corresponding category. Overall, the proposed forecasting approach slightly outperforms the reference methods, by showing small absolute differences in general. In particular, as explained in Section 4.3, the forecasting performance becomes identical to the Marginal for the longer horizon. But for smaller horizons, our approach does better for 4 items, compared to 2 items doing better for Marginal. We naturally cannot draw overarching conclusions based on this evidence.

7 Conclusion

In this work, we considered a multivariate discrete-valued times series model, wherein component count series are obtained by binning the continuous values of latent Gaussian dynamic factor processes. We introduced an estimation method based on second-order properties of the count and latent processes, and PCA. We also suggested additional model selection approaches for determining the number of factor series and their lag orders through cross-validation and information criteria. Facilitated by the state-space formulation of our model, we employed a sequential Monte Carlo method with resampling, for forecasting. Our estimation and forecasting methods were examined on simulated data and an empirical example from psychology.

While our study advances a framework for latent Gaussian time series modeling of categorical observations collected over time, important questions remain. As we pointed out in Remark 3.2, theory for our model in high dimensions is currently being investigated. Regarding estimation, the lag order selection could be improved. There are also potential improvements to make in terms of accuracy and computing time of our forecasting methods. Instead of employing standard particle filtering strategies, one could try other variants of sequential Monte Carlo sampling, for example, ensemble Kalman filtering (e.g. Frei and Künsch, 2013).

Acknowledgement

Vladas Pipiras’s research was partially supported by the grants NSF DMS 1712966, DMS 2113662, and DMS 2134107.

A Kalman recursions and forecasting for SIS/R algorithm

This section describes how the Kalman recursions are used to obtain the h -step-ahead linear prediction of Z_t , $\hat{Z}_{t+h|t} = H_{t1}^{(h)} Z_t + \dots + H_{tt}^{(h)} Z_1$, and how they enter into the SIS/R algorithm. Having the autocovariance function of $\{Z_t\}$, the predictor $\hat{Z}_{t+h|t}$ can naturally be computed through e.g. the Durbin-Levinson algorithm, but the Kalman recursions route provides computational benefit for higher dimension d . Related technical details can be found in Durbin and Koopman (2012), Douc et al. (2014) but this list is not exhaustive.

We consider below the case $p = 1$ only for simplicity. But for higher p , one can convert the $\text{VAR}(p)$ structure of the factor series into an augmented $\text{VAR}(1)$ model by using a companion form of the VAR transition matrix. We define the one-step-ahead prediction of Y_t by $\hat{Y}_{t|t-1}$ when Z_1, \dots, Z_{t-1} are given. Also, we denote the corresponding covariance matrix of prediction error by $\hat{Q}_{t|t-1} := \mathbb{E}[(Y_t - \hat{Y}_{t|t-1})(Y_t - \hat{Y}_{t|t-1})']$. Also, let $\tilde{Y}_{t|t}$ be the filtered estimate and denote the corresponding error covariances $\tilde{Q}_{t|t}$. By convention of Kalman recursions, we let $\tilde{Y}_{0|0} \sim \mathcal{N}(0, \tilde{Q}_{0|0})$ where $\tilde{Q}_{0|0} = \text{Var}(Y_0)$.

The forecast step, which generates the filtering distribution conditioned on the previous information up to $t - 1$, is

$$\hat{Y}_{t|t-1} = \Psi \tilde{Y}_{t-1|t-1} \quad (82)$$

and the corresponding covariance matrix of prediction error is

$$\hat{Q}_{t|t-1} = \Psi \tilde{Q}_{t-1|t-1} \Psi' + \Sigma_\eta. \quad (83)$$

As a consequence, $\hat{Z}_{t|t-1} = \Lambda \hat{Y}_{t|t-1}$ and $\hat{R}_{t|t-1} = \Lambda \hat{Q}_{t|t-1} \Lambda' + \Sigma_\varepsilon$. The joint distribution of the forecast Y_t and Z_t conditioning on $Z_{1:t-1}$ is

$$\begin{pmatrix} Y_t \\ Z_t \end{pmatrix} \Big| Z_{1:t-1} \sim \mathcal{N}_{r+d} \left(\begin{pmatrix} \hat{Y}_{t|t-1} \\ \Lambda \hat{Y}_{t|t-1} \end{pmatrix}, \begin{pmatrix} \hat{Q}_{t|t-1} & \hat{Q}_{t|t-1} \Lambda' \\ \Lambda \hat{Q}_{t|t-1} & \Lambda \hat{Q}_{t|t-1} \Lambda' + \Sigma_\varepsilon \end{pmatrix} \right). \quad (84)$$

From this perspective, one can interpret the update step as sampling Y_t conditioned on $Z_{1:t}$. That is, $Y_t | Z_{1:t} \sim \mathcal{N}_r(\tilde{Y}_{t|t}, \tilde{Q}_{t|t})$ where

$$\tilde{Y}_{t|t} = \hat{Y}_{t|t-1} + K_t(Z_t - \hat{Z}_{t|t-1}), \quad (85)$$

$$\tilde{Q}_{t|t} = (I_r - K_t \Lambda) \hat{Q}_{t|t-1}, \quad (86)$$

where $K_t = \hat{Q}_{t|t-1}\Lambda'(\Lambda\hat{Q}_{t|t-1}\Lambda' + \Sigma_\varepsilon)^{-1} = \hat{Q}_{t|t-1}\Lambda'\hat{R}_{t|t-1}^{-1}$ is called the Kalman gain. The relations (85) and (86) form the update equations for Kalman recursions. One can apply the Sherman-Morrison-Woodbury formula for the matrix inversion of $\hat{R}_{t|t-1}^{-1}$ when the dimension d is high. These two equations are used to update filtered estimators given $Z_{1:t-1}$ when new information about Z_t is added.

Hence, the Kalman recursions for the SIS/R algorithm suggested in Section 4 to obtain one-step-ahead linear prediction $\hat{Z}_{t|t-1}$ are as follows: At each time $t = 1, \dots, T$, carry out the following two steps for $k = 1, \dots, N$,

1. Forecasting step:

$$\hat{Y}_{t|t-1}^{(k)} = \Psi\tilde{Y}_{t|t}^{(k)}, \quad (87)$$

$$\hat{Q}_{t|t-1} = \Psi\tilde{Q}_{t-1|t-1}\Psi' + \Sigma_\eta, \quad (88)$$

$$\hat{Z}_{t|t-1}^{(k)} = \Lambda\hat{Y}_{t|t-1}^{(k)}, \quad (89)$$

$$\hat{R}_{t|t-1} = \Lambda\hat{Q}_{t|t-1}\Lambda' + \Sigma_\varepsilon. \quad (90)$$

4. Updating step:

$$K_t = \hat{Q}_{t|t-1}\Lambda'(\Lambda\hat{Q}_{t|t-1}\Lambda' + \Sigma_\varepsilon)^{-1}, \quad (91)$$

$$\tilde{Y}_{t|t}^{(k)} = \hat{Y}_{t|t-1}^{(k)} + K_t(\tilde{Z}_t^{(k)} - \hat{Z}_{t|t-1}^{(k)}), \quad (92)$$

$$\tilde{Q}_{t|t} = (I_r - K_t\Lambda)\hat{Q}_{t|t-1}. \quad (93)$$

Note that Z_t in (85) is replaced by \tilde{Z}_t in (92) because this is the notation used in the SIS/R algorithm.

Forecasting h -step-ahead linear prediction after T observations in the algorithm is straightforward. Since the latent factor series $\{Y_t\}$ follows a VAR model, the prediction of Y_{T+h} with the information only up to T is

$$\hat{Y}_{T+h|T} = \Psi\hat{Y}_{T+h-1|T} = \dots = \Psi^h\tilde{Y}_{T|T}, \quad (94)$$

and the corresponding covariance matrix of prediction error is

$$\hat{Q}_{T+h|T} = \Psi \hat{Q}_{T+h-1|T} \Psi' + \Sigma_\eta = \dots = \Psi^h \tilde{Q}_{T|T} \Psi^{h'} + \sum_{s=1}^h \Psi^{s-1} \Sigma_\eta \Psi^{s-1'} \quad (95)$$

from (83).

5. Prediction step:

$$\hat{Z}_{T+h|T}^{(k)} = \Lambda \hat{Y}_{T+h|T}^{(k)}, \quad (96)$$

$$\hat{R}_{T+h|T} = \Lambda \hat{Q}_{T+h|T} \Lambda' + \Sigma_\varepsilon. \quad (97)$$

Hence, for each $k = 1, \dots, N$, we compute $\{\hat{Y}_{T+h|T}^{(k)}\}$ as above and then $\hat{Z}_{T+h|T}^{(k)}$ as (96). Likewise, the covariance of the prediction error is also computed by (97). Note that unlike within the observation period, computing (63) is impossible beyond the period. So rather than following Forecasting and Updating steps, we directly compute (96) and (97).

		Bernoulli				Poisson				Negative binomial			
		$\Psi_1^{(1)}$		$\Psi_1^{(2)}$		$\Psi_1^{(1)}$		$\Psi_1^{(2)}$		$\Psi_1^{(1)}$		$\Psi_1^{(2)}$	
$T = 200$		$r = 2$	$r = 5$	$r = 2$	$r = 5$	$r = 2$	$r = 5$	$r = 2$	$r = 5$	$r = 2$	$r = 5$	$r = 2$	$r = 5$
$d = 15$	$L(\hat{\theta})$	0.0983	0.1108	0.0593	0.0561	0.0395	0.0454	0.0182	0.0161	0.0424	0.0490	0.0212	0.0201
	$(B(\hat{\theta}))$	(0.0932)	(0.1033)	(0.0532)	(0.0505)	(0.0414)	(0.0472)	(0.0188)	(0.0172)	(0.0397)	(0.0449)	(0.0181)	(0.0173)
	$L(\hat{\Lambda})$	0.2359	0.9250	0.2454	0.4097	0.2526	0.4013	0.2430	0.3602	0.2008	0.2149	0.2068	0.2048
	$(B(\hat{\Lambda}))$	(0.2096)	(0.8135)	(0.2184)	(0.3630)	(0.2208)	(0.3453)	(0.2166)	(0.3141)	(0.1773)	(0.1906)	(0.1816)	(0.1825)
	$L(\hat{\Sigma}_e)$	0.1941	0.4051	0.2004	0.3925	0.1917	0.4341	0.1911	0.4313	0.2712	0.3942	0.2826	0.3930
	$(B(\hat{\Sigma}_e))$	(2.0266)	(2.7742)	(2.0074)	(2.7189)	(1.8552)	(2.4232)	(1.8289)	(2.3533)	(1.5820)	(2.3429)	(1.5647)	(2.3379)
	$L(\hat{\Psi})$	0.2610	1.0902	0.2930	0.5178	0.2677	0.5113	0.2589	0.5369	0.1916	0.4097	0.2837	0.5283
	$(B(\hat{\Psi}))$	(0.3236)	(1.9506)	(0.3640)	(0.9261)	(0.3351)	(0.8686)	(0.3215)	(0.9093)	(0.2352)	(0.7416)	(0.3581)	(0.9220)
	$L(\hat{\Sigma}_\eta)$	0.5151	1.0362	0.5985	1.0143	0.4549	1.0387	0.5093	1.1049	0.4025	0.9454	0.6550	1.4207
	$(B(\hat{\Sigma}_\eta))$	(0.6519)	(1.8660)	(0.7575)	(1.8326)	(0.5737)	(1.8403)	(0.6384)	(1.9264)	(0.5135)	(1.7314)	(0.8379)	(2.4169)
$d = 30$	$L(\hat{\theta})$	0.0885	0.1067	0.0590	0.0561	0.0334	0.0431	0.0182	0.0151	0.0377	0.0473	0.0216	0.0194
	$(B(\hat{\theta}))$	(0.0821)	(0.0990)	(0.0523)	(0.0499)	(0.0349)	(0.0444)	(0.0185)	(0.0158)	(0.0345)	(0.0437)	(0.0185)	(0.0165)
	$L(\hat{\Lambda})$	0.2312	0.0799	0.2334	0.3507	0.2276	0.3870	0.2258	0.3481	0.1944	0.2295	0.1889	0.2185
	$(B(\hat{\Lambda}))$	(0.2021)	(0.2108)	(0.2031)	(0.3259)	(0.1889)	(0.3471)	(0.1891)	(0.3143)	(0.1704)	(0.2140)	(0.1657)	(0.2053)
	$L(\hat{\Sigma}_e)$	0.3200	0.3872	0.3251	0.8346	0.2736	0.6404	0.2658	0.5595	0.2266	0.6708	0.2256	0.6788
	$(B(\hat{\Sigma}_e))$	(2.9930)	(2.3327)	(2.9290)	(4.9342)	(2.7494)	(4.2943)	(2.7214)	(4.0931)	(2.1924)	(3.7540)	(2.1633)	(3.7733)
	$L(\hat{\Psi})$	0.4482	0.3427	0.5304	0.7006	0.3319	0.5390	0.4366	0.5396	0.3968	0.6264	0.6843	0.9246
	$(B(\hat{\Psi}))$	(0.5725)	(0.6004)	(0.6893)	(1.2840)	(0.4198)	(0.9555)	(0.5566)	(0.9667)	(0.4814)	(1.1103)	(0.8138)	(1.5611)
	$L(\hat{\Sigma}_\eta)$	0.9443	0.9281	1.1559	1.3647	0.6980	0.9251	0.9345	0.9931	0.9480	1.6445	1.8266	2.8432
	$(B(\hat{\Sigma}_\eta))$	(1.2144)	(1.6720)	(1.4959)	(2.4750)	(0.8890)	(1.6413)	(1.2112)	(1.7826)	(1.1630)	(2.8619)	(2.1791)	(4.7215)
$T = 400$		$r = 2$	$r = 5$	$r = 2$	$r = 5$	$r = 2$	$r = 5$	$r = 2$	$r = 5$	$r = 2$	$r = 5$	$r = 2$	$r = 5$
$d = 15$	$L(\hat{\theta})$	0.0726	0.0799	0.0430	0.0390	0.0291	0.0326	0.0131	0.0106	0.0313	0.0355	0.0146	0.0135
	$(B(\hat{\theta}))$	(0.0679)	(0.0745)	(0.0384)	(0.0353)	(0.0306)	(0.0339)	(0.0133)	(0.0114)	(0.0292)	(0.0324)	(0.0125)	(0.0118)
	$L(\hat{\Lambda})$	0.1602	0.3631	0.1639	0.2264	0.1817	0.2362	0.1712	0.2130	0.1743	0.1557	0.1727	0.1488
	$(B(\hat{\Lambda}))$	(0.1406)	(0.3385)	(0.1448)	(0.1984)	(0.1604)	(0.2075)	(0.1501)	(0.1847)	(0.1527)	(0.1379)	(0.1508)	(0.1319)
	$L(\hat{\Sigma}_e)$	0.1771	0.8207	0.1428	0.3957	0.1510	0.3816	0.1466	0.3872	0.3097	0.3882	0.3102	0.3910
	$(B(\hat{\Sigma}_e))$	(2.6476)	(4.9094)	(1.6892)	(2.3312)	(1.6019)	(2.2172)	(1.5932)	(2.1589)	(1.4207)	(2.2613)	(1.4172)	(2.2545)
	$L(\hat{\Psi})$	0.2482	0.6421	0.1788	0.3484	0.1920	0.3369	0.2084	0.3686	0.1401	0.3079	0.2115	0.4795
	$(B(\hat{\Psi}))$	(0.3184)	(1.1707)	(0.2215)	(0.6092)	(0.2364)	(0.5866)	(0.2565)	(0.6316)	(0.1725)	(0.5697)	(0.2740)	(0.8195)
	$L(\hat{\Sigma}_\eta)$	0.5236	1.2595	0.3671	0.9311	0.3777	0.9154	0.4460	0.9653	0.3325	0.7859	0.4720	1.3329
	$(B(\hat{\Sigma}_\eta))$	(0.6832)	(2.2496)	(0.4641)	(1.6363)	(0.4793)	(1.6014)	(0.5568)	(1.6852)	(0.4219)	(1.4857)	(0.6102)	(2.2414)
$d = 30$	$L(\hat{\theta})$	0.0662	0.0758	0.0419	0.0402	0.0253	0.0312	0.0131	0.0108	0.0283	0.0341	0.0147	0.0135
	$(B(\hat{\theta}))$	(0.0616)	(0.0705)	(0.0373)	(0.0358)	(0.0265)	(0.0323)	(0.0132)	(0.0112)	(0.0260)	(0.0314)	(0.0125)	(0.0116)
	$L(\hat{\Lambda})$	0.1602	0.2343	0.1612	0.2284	0.1517	0.2190	0.1510	0.2020	0.1549	0.1683	0.1550	0.1669
	$(B(\hat{\Lambda}))$	(0.1406)	(0.2176)	(0.1399)	(0.2126)	(0.1272)	(0.1985)	(0.1260)	(0.1843)	(0.1372)	(0.1588)	(0.1371)	(0.1573)
	$L(\hat{\Sigma}_e)$	0.1771	0.6167	0.1781	0.6541	0.1339	0.3463	0.1261	0.2828	0.1961	0.6337	0.1945	0.6422
	$(B(\hat{\Sigma}_e))$	(2.6476)	(4.2705)	(2.5933)	(4.3563)	(2.3694)	(3.3760)	(2.3614)	(3.1930)	(1.8801)	(3.5548)	(1.8734)	(3.5736)
	$L(\hat{\Psi})$	0.2482	0.4082	0.2563	0.4544	0.1598	0.2874	0.1636	0.2814	0.3194	0.5508	0.5773	0.8636
	$(B(\hat{\Psi}))$	(0.3184)	(0.7532)	(0.3372)	(0.8547)	(0.2020)	(0.5144)	(0.2075)	(0.4954)	(0.4014)	(0.9661)	(0.6772)	(1.4011)
	$L(\hat{\Sigma}_\eta)$	0.5236	0.8403	0.5701	0.9375	0.3074	0.5790	0.3288	0.6026	0.7529	1.4064	1.4893	2.5581
	$(B(\hat{\Sigma}_\eta))$	(0.6832)	(1.5391)	(0.7475)	(1.7420)	(0.3966)	(1.0495)	(0.4233)	(1.0797)	(0.9531)	(2.4295)	(1.7575)	(4.1353)

Table 1: The ℓ_2 losses ($L(\cdot)$) and biases ($B(\cdot)$) for various combinations of model parameters including transition matrices Ψ , number of factors r , number of time points T , dimension d , and several marginal distributions.

Bernoulli			Forecasting horizon											
			h = 1		h = 2		h = 3		h = 4		h = 5			
Ψ	d	r	RMFE _y	RMFE _z	RMFE _y	RMFE _z	RMFE _y	RMFE _z	RMFE _y	RMFE _z	RMFE _y	RMFE _z	RMFE _y	RMFE _z
$\Psi^{(1)}$	15	2	0.6804	0.2341	0.3673	0.7200 (0.674,0.6700)	0.7671	0.2452	0.4110	0.724 (0.693,0.6480)	0.7307	0.2484	0.4119	0.734 (0.6973,0.6373)
$\Psi^{(1)}$	15	5	0.4922	0.2318	0.3647	0.7360 (0.680,0.7233)	0.4951	0.2396	0.3890	0.7307 (0.673,0.6847)	0.5078	0.2430	0.4784	0.6973 (0.6687,0.6027)
$\Psi^{(1)}$	30	2	0.6945	0.1665	0.3329	0.7363 (0.6727,0.6743)	0.7408	0.1702	0.4086	0.7117 (0.665,0.6467)	0.7994	0.1816	0.3916	0.7137 (0.682,0.6863)
$\Psi^{(1)}$	30	5	0.4670	0.1586	0.3352	0.7437 (0.6670,0.7140)	0.5005	0.1705	0.4026	0.7303 (0.6740,0.6770)	0.5261	0.1816	0.4634	0.7087 (0.6723,0.6467)
$\Psi^{(2)}$	15	2	0.6827	0.2383	0.3628	0.7295 (0.6840,0.7293)	0.8027	0.2538	0.4395	0.6993 (0.6720,0.6373)	0.8010	0.2394	0.4846	0.6993 (0.6860,0.6393)
$\Psi^{(2)}$	15	5	0.4722	0.2223	0.3687	0.7235 (0.6833,0.7077)	0.5313	0.2460	0.4215	0.7207 (0.6913,0.7020)	0.5315	0.2369	0.4535	0.7053 (0.6853,0.6353)
$\Psi^{(2)}$	30	2	0.7232	0.1750	0.4427	0.7067 (0.6633,0.6940)	0.7819	0.1792	0.3762	0.7207 (0.6837,0.6663)	0.7643	0.1795	0.4877	0.6910 (0.6717,0.5403)
$\Psi^{(2)}$	30	5	0.4674	0.1596	0.3708	0.7447 (0.6880,0.6973)	0.5239	0.1720	0.3993	0.7053 (0.6653,0.6820)	0.5237	0.1789	0.4976	0.6967 (0.6893,0.6327)
Poisson														
$\Psi^{(1)}$	15	2	0.6628	0.2353	0.0153	0.5107 (0.4520,0.4540)	0.7413	0.2500	0.0216	0.4807 (0.4333,0.4447)	0.7948	0.2270	0.0216	0.4807 (0.4447,0.4287)
$\Psi^{(1)}$	15	5	0.4448	0.2141	0.0146	0.5267 (0.4400,0.4993)	0.4927	0.2380	0.0210	0.4807 (0.4380,0.4553)	0.5068	0.2424	0.0210	0.4833 (0.4353,0.4313)
$\Psi^{(1)}$	30	2	0.6912	0.1598	0.0149	0.5067 (0.4447,0.4473)	0.7392	0.1695	0.0166	0.4870 (0.4390,0.4287)	0.7919	0.1686	0.0168	0.4870 (0.4370,0.4270)
$\Psi^{(1)}$	30	5	0.4236	0.1497	0.0156	0.5130 (0.4493,0.4717)	0.4983	0.1647	0.0172	0.4947 (0.4473,0.4440)	0.4854	0.1664	0.0168	0.4947 (0.4500,0.4393)
$\Psi^{(2)}$	15	2	0.6948	0.2390	0.0184	0.4967 (0.4667,0.4620)	0.6986	0.2368	0.0191	0.4917 (0.4440,0.4493)	0.7132	0.2402	0.0190	0.4967 (0.4780,0.4120)
$\Psi^{(2)}$	15	5	0.4430	0.2122	0.0157	0.5120 (0.4593,0.3867)	0.4697	0.2299	0.0178	0.4587 (0.4353,0.4663)	0.5188	0.2413	0.0219	0.4587 (0.4320,0.3880)
$\Psi^{(2)}$	30	2	0.6348	0.1622	0.0170	0.4987 (0.4430,0.3963)	0.7400	0.1734	0.0162	0.4790 (0.4367,0.4474)	0.7534	0.1746	0.0197	0.4917 (0.4533,0.3890)
$\Psi^{(2)}$	30	5	0.4156	0.1522	0.0184	0.5120 (0.4507,0.3983)	0.4811	0.1675	0.0180	0.4953 (0.4490,0.4580)	0.5167	0.1666	0.0181	0.4967 (0.4657,0.3960)
Negative binomial														
$\Psi^{(1)}$	15	2	0.6555	0.2360	0.0296	0.1967 (0.1417,0.1673)	0.7716	0.2378	0.0308	0.1933 (0.1433,0.1420)	0.8088	0.2548	0.0345	0.2040 (0.1600,0.1453)
$\Psi^{(1)}$	15	5	0.4390	0.2135	0.0244	0.2373 (0.1627,0.1967)	0.4862	0.2287	0.0284	0.2153 (0.1480,0.1620)	0.4999	0.2411	0.0278	0.2153 (0.1587,0.1473)
$\Psi^{(1)}$	30	2	0.6900	0.1616	0.0258	0.2063 (0.1463,0.1703)	0.7220	0.1718	0.0283	0.2067 (0.1580,0.1523)	0.7520	0.1808	0.0331	0.1893 (0.1633,0.1420)
$\Psi^{(1)}$	30	5	0.4021	0.1470	0.0256	0.2283 (0.1523,0.184)	0.4986	0.1607	0.0298	0.2043 (0.1560,0.1527)	0.5141	0.1755	0.0290	0.2103 (0.1560,0.1527)
$\Psi^{(2)}$	15	2	0.6048	0.2356	0.0260	0.1927 (0.1300,0.1200)	0.6817	0.2444	0.0347	0.1833 (0.1487,0.1067)	0.6997	0.2435	0.0326	0.1833 (0.1487,0.1067)
$\Psi^{(2)}$	15	5	0.4426	0.2222	0.0256	0.2287 (0.1793,0.0913)	0.5306	0.2385	0.0316	0.2087 (0.1547,0.1107)	0.5171	0.2529	0.0363	0.1718 (0.1353,0.1320)
$\Psi^{(2)}$	30	2	0.6315	0.1596	0.0277	0.2059 (0.1653,0.1140)	0.7386	0.1740	0.0314	0.1943 (0.1523,0.1493)	0.7928	0.1797	0.0387	0.1937 (0.1520,0.1273)
$\Psi^{(2)}$	30	5	0.387	0.1481	0.0292	0.2033 (0.1473,0.090)	0.4545	0.1621	0.0278	0.2117 (0.1623,0.1600)	0.4991	0.1736	0.0309	0.2040 (0.1643,0.0514)

Table 2: The h -step forecasting error measures at the observation level and the two latent process levels for various combinations of model parameters including transition matrices Ψ , number of factors r , dimension d , and several marginal distributions. Sample size T is fixed as 200. (L, M) refers to sensitivities from Last observation and Marginal likelihood predictions, respectively.

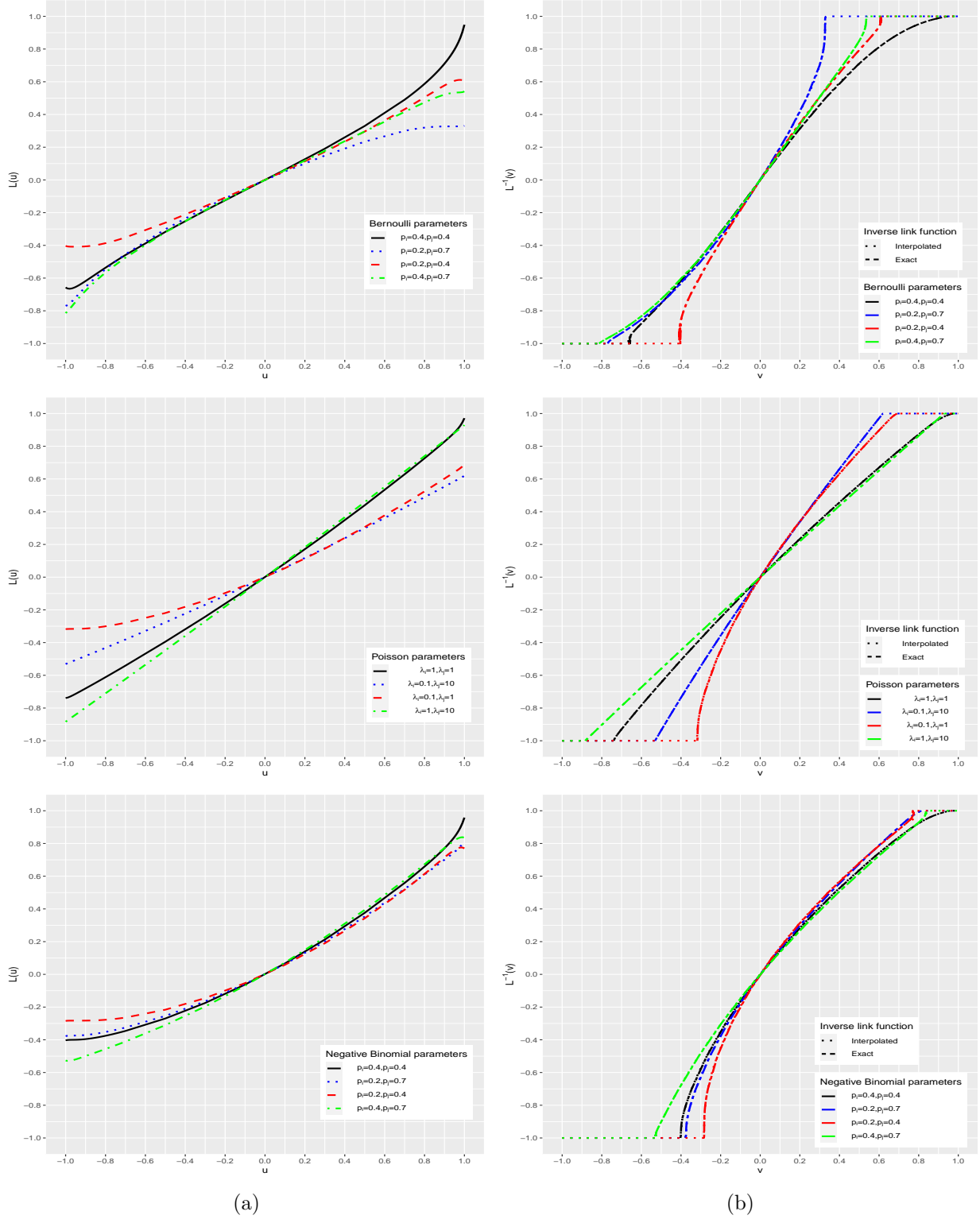


Figure 1: (a) The link function $L_{ij}(u)$ for several combinations of CDFs $F_i = \text{Bern}(p_i)$, $F_i = \text{Pois}(\lambda_i)$, and $F_i = \text{NB}(r, p_i)$ with $r = 3$ (same type of distribution for j). (b) The inverse link function $L_{ij}^{-1}(v)$ and its interpolation $\tilde{L}_{ij}^{-1}(v)$ for chosen combinations of CDFs.

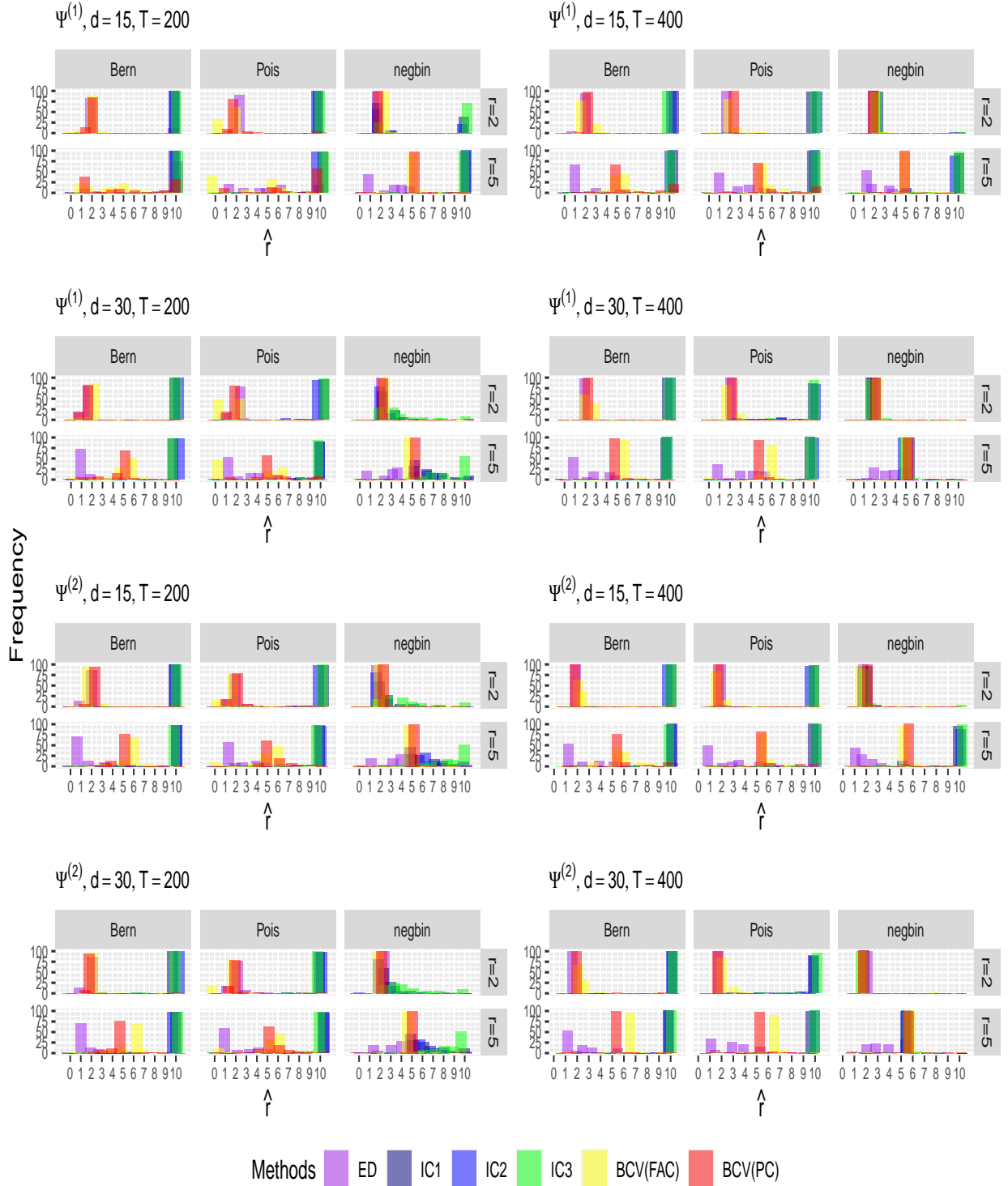


Figure 2: Estimated number of factors from simulated data for various combinations of model parameters including transition matrices Ψ , number of factors r , number of time points T , dimension d , and several marginal distributions.

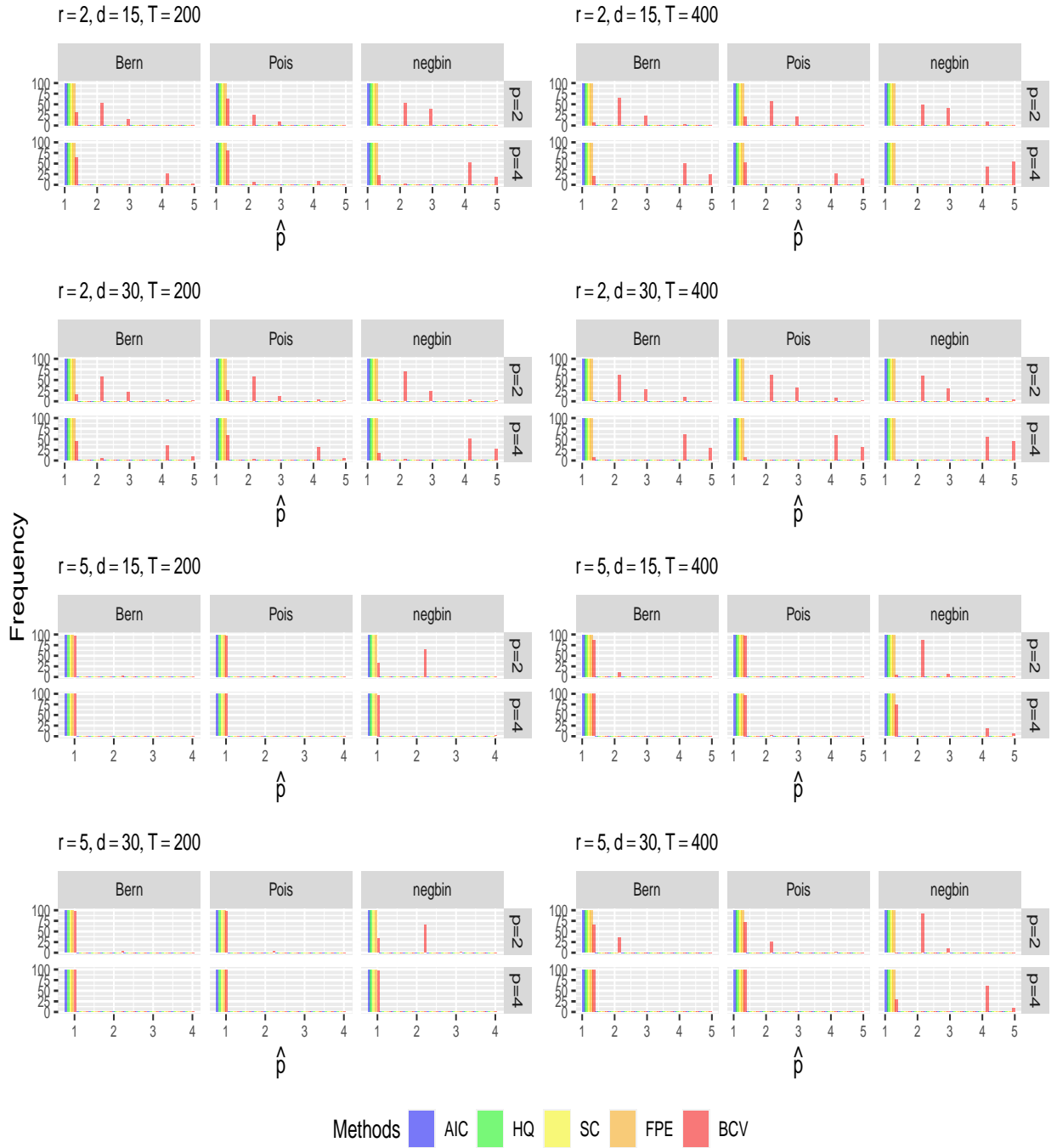


Figure 3: Estimated lag order from simulated data for various combinations of model parameters including transition matrices with different lag order p , number of factors r , number of time points T , dimension d , and several marginal distributions.

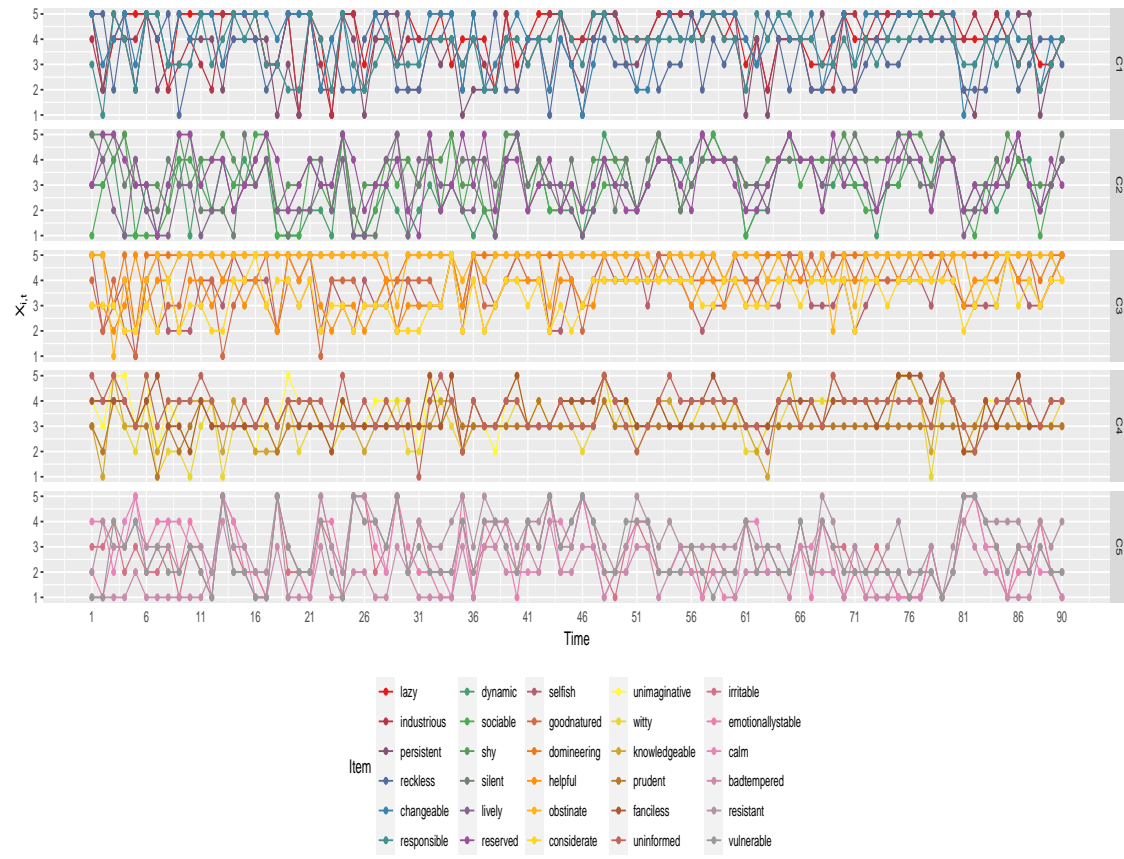


Figure 4: Time plots of 90-day observations for 30 items.

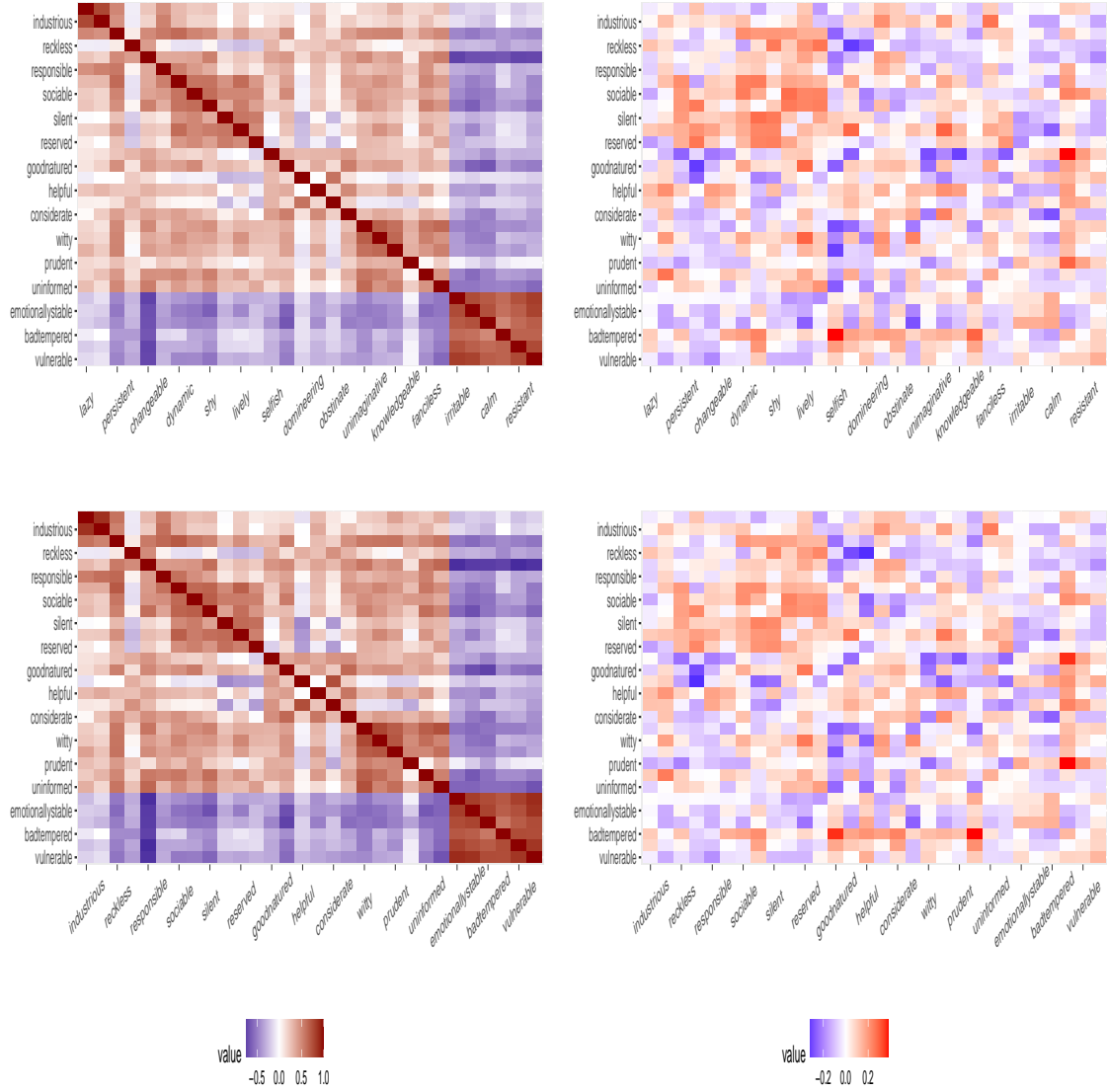


Figure 5: (Top) The sample autocorrelation matrices of the observations at lag 0 (left) and lag 1 (right), $\hat{\Sigma}_X(h)$, $h = 0, 1$. (Bottom) The estimated autocorrelation matrices of the latent Gaussian series at lag 0 (left) and lag 1 (right), $\hat{\Sigma}_Z(h)$, $h = 0, 1$.

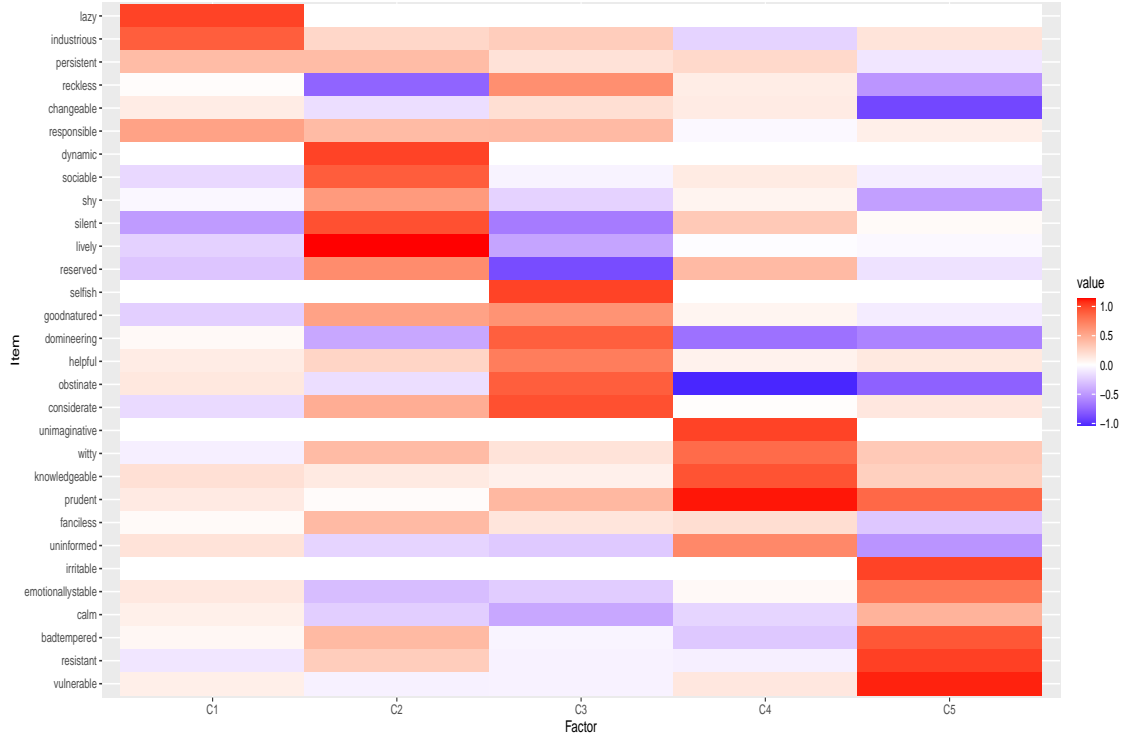


Figure 6: Estimate of the loadings matrix $\hat{\Lambda}$.

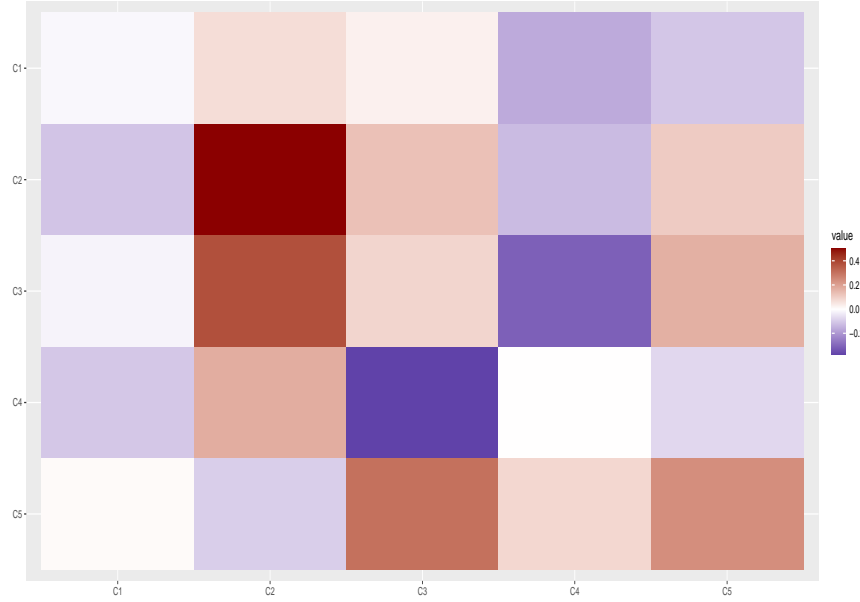


Figure 7: Estimate of the VAR(1) transition matrix $\hat{\Psi}_1$.

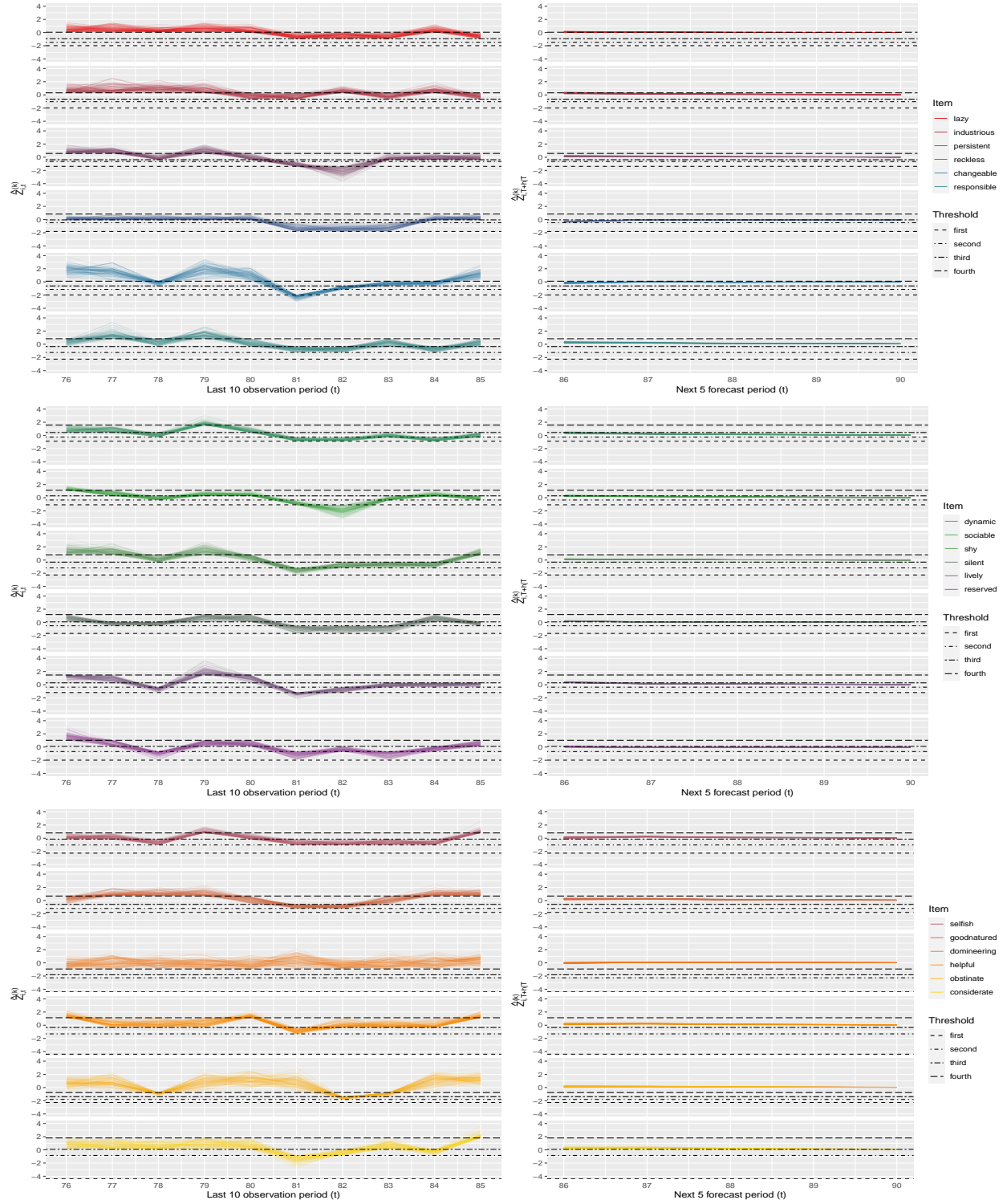


Figure 8: The simulated particles for the first 18 items in the observation period (left) and forecasting period (right). Two consecutive horizontal lines with different line types form the bin for discrete observations of each item.

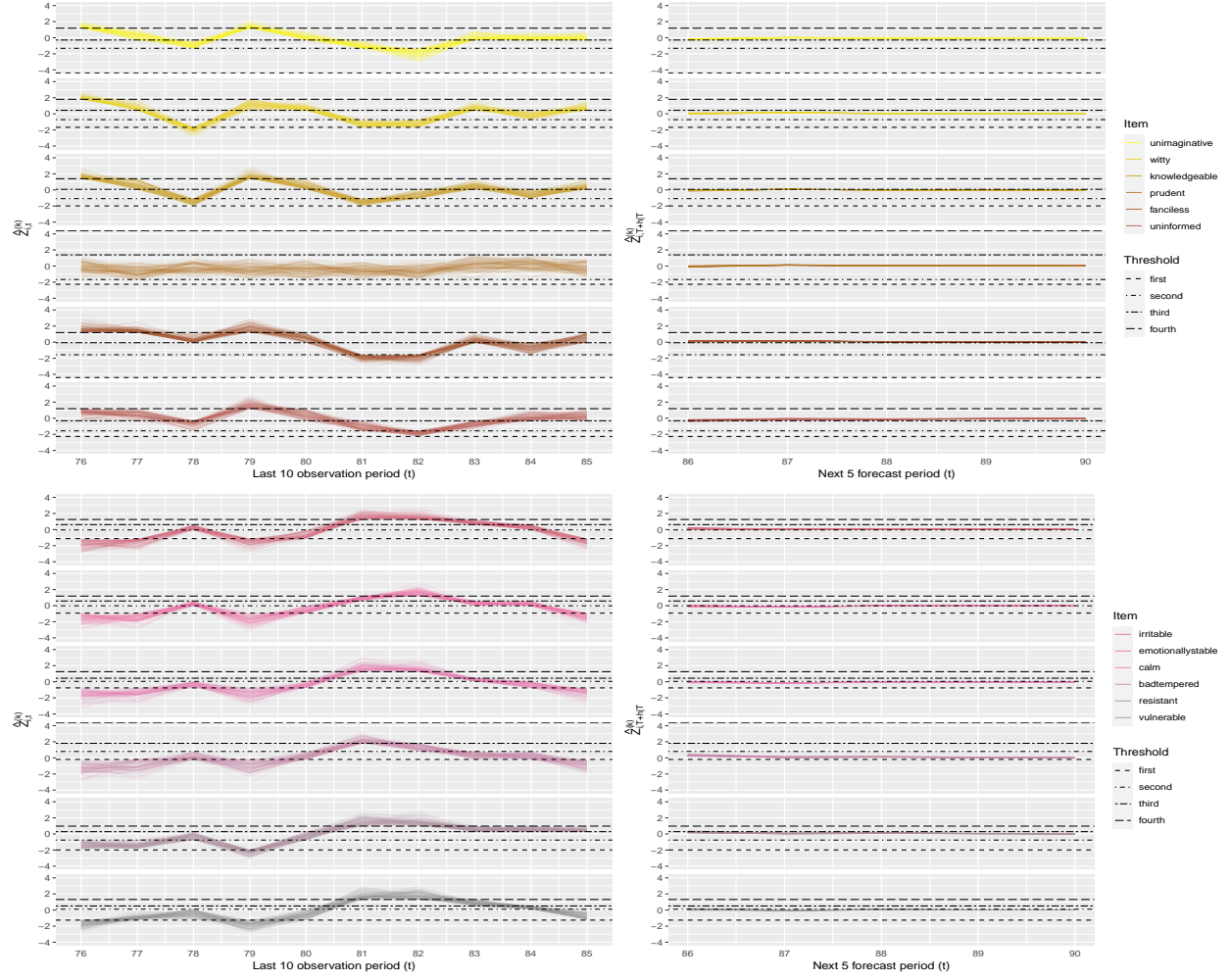


Figure 9: The simulated particles for the next 12 items in the observation period (left) and forecasting period (right). Two consecutive lines with different line types form the bin for discrete observations of each item.

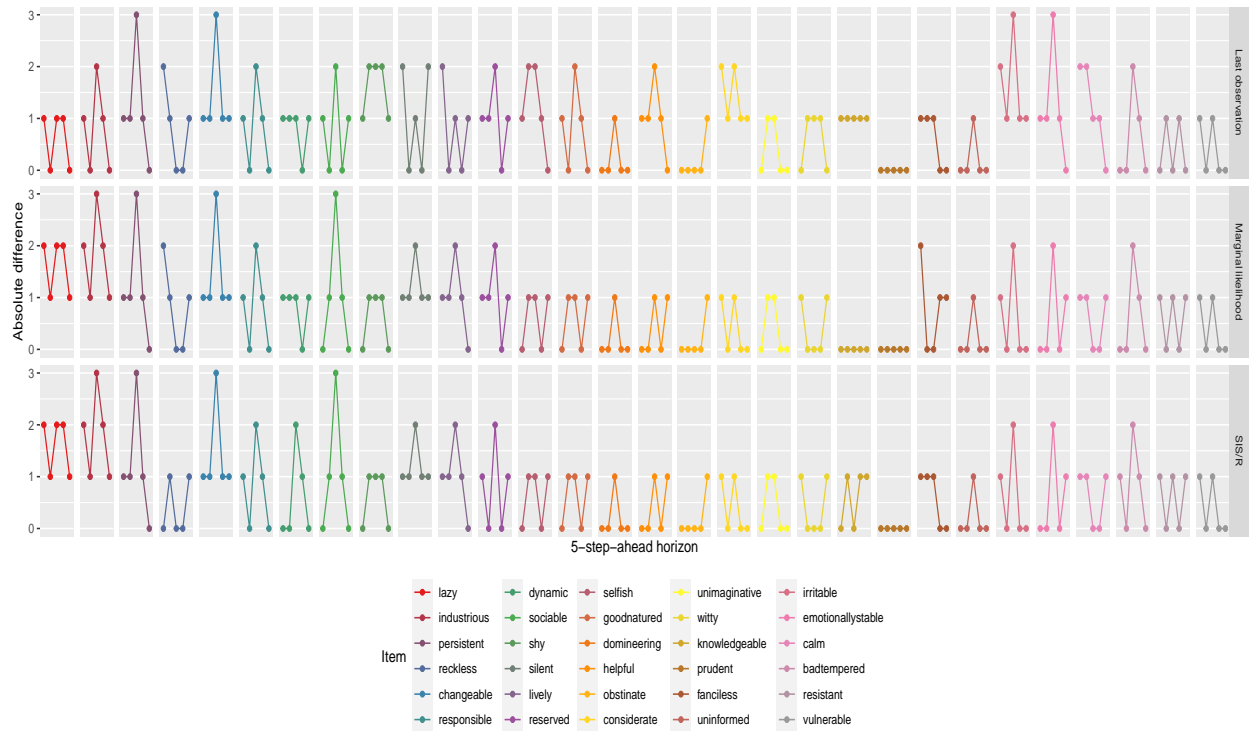


Figure 10: Result of 5-step-ahead prediction of each item with two baseline approaches. Each of 6 items in order are known to be affected by the same category.

References

- Alzaid, A. A. and Al-Osh, M. A. (1993). Some autoregressive moving average processes with generalized Poisson marginal distributions. *Annals of the Institute of Statistical Mathematics*, 45(2):223–232.
- Andrieu, C. and Doucet, A. (2002). Particle filtering for partially observed Gaussian state space models. *Journal of the Royal Statistical Society: Series B (Statistical Methodology)*, 64(4):827–836.
- Bai, J. and Ng, S. (2002). Determining the number of factors in approximate factor models. *Econometrica*, 70(1):191–221.
- Bai, J. and Wang, P. (2015). Identification and Bayesian estimation of dynamic factor models. *Journal of Business & Economic Statistics*, 33(2):221–240.
- Bertsimas, D., Copenhaver, M. S., and Mazumder, R. (2017). Certifiably optimal low rank factor analysis. *The Journal of Machine Learning Research*, 18(1):907–959.
- Borkenau, P. and Ostendorf, F. (1998). The Big Five as states: How useful is the five-factor model to describe intraindividual variations over time? *Journal of Research in Personality*, 32(2):202–221.
- Bräuning, F. and Koopman, S. J. (2020). The dynamic factor network model with an application to international trade. *Journal of Econometrics*, 216(2):494–515.
- Briers, M., Doucet, A., and Maskell, S. (2010). Smoothing algorithms for state-space models. *Annals of the Institute of Statistical Mathematics*, 62(1):61–89.
- Browne, M. W. and Cudeck, R. (1989). Single sample cross-validation indices for covariance structures. *Multivariate Behavioral Research*, 24(4):445–455.
- Chen, S., Shojaie, A., Shea-Brown, E., and Witten, D. (2017). The multivariate Hawkes process in high dimensions: Beyond mutual excitation. *arXiv preprint arXiv:1707.04928*.
- Cui, K. and Dunson, D. B. (2014). Generalized dynamic factor models for mixed-measurement time series. *Journal of Computational and Graphical Statistics*, 23(1):169–191.
- Davis, R. A., Fokianos, K., Holan, S. H., Joe, H., Livsey, J., Lund, R., Pipiras, V., and Ravishanker, N. (2021). Count time series: A methodological review. *Journal of the American Statistical Association*, 116(535):1533–1547.
- Davis, R. A., Holan, S. H., Lund, R., and Ravishanker, N. (2016). *Handbook of Discrete-Valued Time Series*. CRC Press.

- Douc, R. and Cappé, O. (2005). Comparison of resampling schemes for particle filtering. In *ISPA 2005. Proceedings of the 4th International Symposium on Image and Signal Processing and Analysis, 2005.*, pages 64–69. IEEE.
- Douc, R., Moulines, E., and Stoffer, D. (2014). *Nonlinear Time Series: Theory, Methods and Applications with R Examples*. CRC press.
- Doucet, A., de Freitas, N., and Gordon, N. (2001). An introduction to sequential Monte Carlo methods. In *Sequential Monte Carlo Methods in Practice*, pages 3–14. Springer New York.
- Doucet, A. and Johansen, A. M. (2009). A tutorial on particle filtering and smoothing: Fifteen years later. In *Handbook of Nonlinear Filtering*, volume 12, pages 656–704.
- Düker, M.-C., Lund, R., and Pipiras, V. (2023). High-dimensional latent Gaussian count time series: Concentration results for autocovariances and applications. *arXiv preprint arXiv:2301.00491*.
- Durbin, J. and Koopman, S. J. (2012). *Time Series Analysis by State Space Methods*. Oxford University Press.
- Ferland, R., Latour, A., and Oraichi, D. (2006). Integer-valued GARCH process. *Journal of Time Series Analysis*, 27(6):923–942.
- Fokianos, K., Rahbek, A., and Tjøstheim, D. (2009). Poisson autoregression. *Journal of the American Statistical Association*, 104(488):1430–1439.
- Fokianos, K., Støve, B., Tjøstheim, D., Doukhan, P., et al. (2020). Multivariate count autoregression. *Bernoulli*, 26(1):471–499.
- Forni, M., Hallin, M., Lippi, M., and Reichlin, L. (2000). The generalized dynamic-factor model: Identification and estimation. *Review of Economics and Statistics*, 82(4):540–554.
- Forni, M., Hallin, M., Lippi, M., and Reichlin, L. (2005). The generalized dynamic factor model: one-sided estimation and forecasting. *Journal of the American Statistical Association*, 100(471):830–840.
- Frei, M. and Künsch, H. R. (2013). Bridging the ensemble Kalman and particle filters. *Biometrika*, 100(4):781–800.
- Gamerman, D., Abanto-Valle, C. A., Silva, R. S., and Martins, T. G. (2016). Dynamic Bayesian models for discrete-valued time series. In *Handbook of Discrete-Valued Time Series*, pages 165–186. Chapman and Hall/CRC.
- Hall, E. C., Raskutti, G., and Willett, R. M. (2018). Learning high-dimensional generalized linear autoregressive models. *IEEE Transactions on Information Theory*, 65(4):2401–2422.

- Harman, H. H. and Jones, W. H. (1966). Factor analysis by minimizing residuals (MINRES). *Psychometrika*, 31(3):351–368.
- Haslbeck, J. and van Bork, R. (2022). Estimating the number of factors in exploratory factor analysis via out-of-sample prediction errors. *Psychological Methods*.
- Jia, Y., Kechagias, S., Livsey, J., Lund, R., and Pipiras, V. (2023). Latent Gaussian count time series. *Journal of the American Statistical Association*, 118(541):596–606.
- Jung, R. C., Liesenfeld, R., and Richard, J.-F. (2011). Dynamic factor models for multivariate count data: An application to stock-market trading activity. *Journal of Business & Economic Statistics*, 29(1):73–85.
- Kachour, M. and Truquet, L. (2011). A p -order signed integer-valued autoregressive (SINAR (p)) model. *Journal of Time Series Analysis*, 32(3):223–236.
- Karlis, D. (2016). Models for multivariate count time series. In *Handbook of Discrete-Valued Time Series*, pages 407–424. Chapman and Hall/CRC.
- Kim, H.-Y. and Park, Y. (2008). A non-stationary integer-valued autoregressive model. *Statistical Papers*, 49(3):485–502.
- Kong, J. and Lund, R. (2023). Seasonal count time series. *Journal of Time Series Analysis*, 44(1):93–124.
- Kress, R. (1998). *Numerical Analysis*, volume 181. Springer Science & Business Media.
- Lebo, M. A. and Nesselroade, J. R. (1978). Intraindividual differences dimensions of mood change during pregnancy identified in five p-technique factor analyses. *Journal of Research in Personality*, 12(2):205–224.
- Lütkepohl, H. (2005). *New Introduction to Multiple Time Series Analysis*. Springer Science & Business Media.
- Mark, B., Raskutti, G., and Willett, R. (2018). Network estimation from point process data. *IEEE Transactions on Information Theory*, 65(5):2953–2975.
- Mark, B., Raskutti, G., and Willett, R. (2019). Estimating network structure from incomplete event data. In *The 22nd International Conference on Artificial Intelligence and Statistics*, pages 2535–2544. PMLR.
- McKenzie, E. (1985). Some simple models for discrete variate time series. *JAWRA Journal of the American Water Resources Association*, 21(4):645–650.
- Muthén, B. (1984). A general structural equation model with dichotomous, ordered categorical, and continuous latent variable indicators. *Psychometrika*, 49(1):115–132.

- Onatski, A. (2010). Determining the number of factors from empirical distribution of eigenvalues. *The Review of Economics and Statistics*, 92(4):1004–1016.
- Pipiras, V. and Taqqu, M. S. (2017). *Long-Range Dependence and Self-Similarity*, volume 45. Cambridge University Press.
- Revelle, W. (2023). *psych: Procedures for Psychological, Psychometric, and Personality Research*. R package version 2.3.3.
- Robitzsch, A. (2020). Why ordinal variables can (almost) always be treated as continuous variables: Clarifying assumptions of robust continuous and ordinal factor analysis estimation methods. *Frontiers in Education*.
- Rosseel, Y. (2012). lavaan: An R package for structural equation modeling. *Journal of Statistical Software*, 48(2):1–36.
- Snyder, C., Bengtsson, T., Bickel, P., and Anderson, J. (2008). Obstacles to high-dimensional particle filtering. *Monthly Weather Review*, 136(12):4629–4640.
- Wang, F. and Wang, H. (2018). Modelling non-stationary multivariate time series of counts via common factors. *Journal of the Royal Statistical Society: Series B (Statistical Methodology)*, 80(4):769–791.
- Wei, C. H. (2018). *An Introduction to Discrete-Valued Time Series*. John Wiley & Sons.
- Whitt, W. (1976). Bivariate distributions with given marginals. *The Annals of Statistics*, 4(6):1280–1289.
- Wilhelm, S. and Manjunath, B. G. (2010). tmvtnorm: A Package for the Truncated Multivariate Normal Distribution. *The R Journal*, 2(1):25–29.
- Zhang, G. and Browne, M. W. (2010). Dynamic factor analysis with ordinal manifest variables. In *Statistical methods for modeling human dynamics: An interdisciplinary dialogue*, pages 241–263. Routledge/Taylor & Francis Group.
- Zhang, H., Wang, D., and Zhu, F. (2010). Inference for INAR (p) processes with signed generalized power series thinning operator. *Journal of Statistical Planning and Inference*, 140(3):667–683.
- Zhang, Z. and Nesselroade, J. R. (2007). Bayesian estimation of categorical dynamic factor models. *Multivariate Behavioral Research*, 42(4):729–756.